DEUTSCHES ELEKTRONEN-SYNCHROTRON DESY

Recent Results from DORIS

by

B. H. Wiik

To be sure that your preprints are promptly included in the
HIGH ENERGY PHYSICS INDEX,
send them to the following address (if possible by air mail) :

B. H. Wiik: Recent Results from DORIS.

The following footnote was omitted from the title page:
Invited talk at the International Symposium on Lepton and Hadron Interactions,
Stanford University, Stanford, California, August 21-27, 1975.

The data from the DASP-Collaboration presented in this report should be
quoted:

DASP-Collaboration: B. H. Wiik, Invited talk at the International
Symposium on Lepton and Photon Interactions, Stanford University, Stanford,
California, August 21-27, 1975.

RECENT RESULTS FROM DORIS

B.H.Wiik

Deutsches Elektronen-Synchrotron DESY, Hamburg, Germany

The experimental program utilizing the e^+e^- colliding ring DORIS got under-way in late 1974. Since then data have been taken using three large, rather complementary detectors. In this talk the present status of the accelerator will be described and the data obtained with the double arm spectrometer DASP and the superconducting solenoid PLUTO discussed. The results obtained with the third detector will be shown by Prof. Heintze.

Most of the data have been collected for energies at or adjacent to the masses of the newly found resonances[1] at 3.09 GeV and 3.68 GeV. Here pre-liminary results on the following topics will be presented:

1) Inclusive distributions, particle ratios, and limits on heavy charged mesons from the decays of the J/ψ and ψ' resonances.

2) Hadronic two body decays of J/ψ and ψ'.

3) The cascade decay: $\psi' \rightarrow (J/\psi) + X$.

4) Evidence for narrow states P_c with even charge conjugation and masses between 3.7 GeV and 3.1 GeV.

5) Two photon final states.

6) Three photon final states and evidence for a new resonance.

The results on the decay of the resonances into lepton pairs[2] agree within the errors with the data reported by the SPEAR solenoid group[3] and will not be discussed here.

DORIS

The layout of the DESY accelerator complex is shown in Fig. 1. Electrons and positrons from a 400 MeV linear accelerator are injected into the 7.5 GeV synchrotron to be accelerated to the proper energy for transfer to DORIS. DORIS is in the shape of a race track with two nearly indepen-dent rings stacked one above the other. The beams cross in the vertical plane in the middle of the two long straight sections.
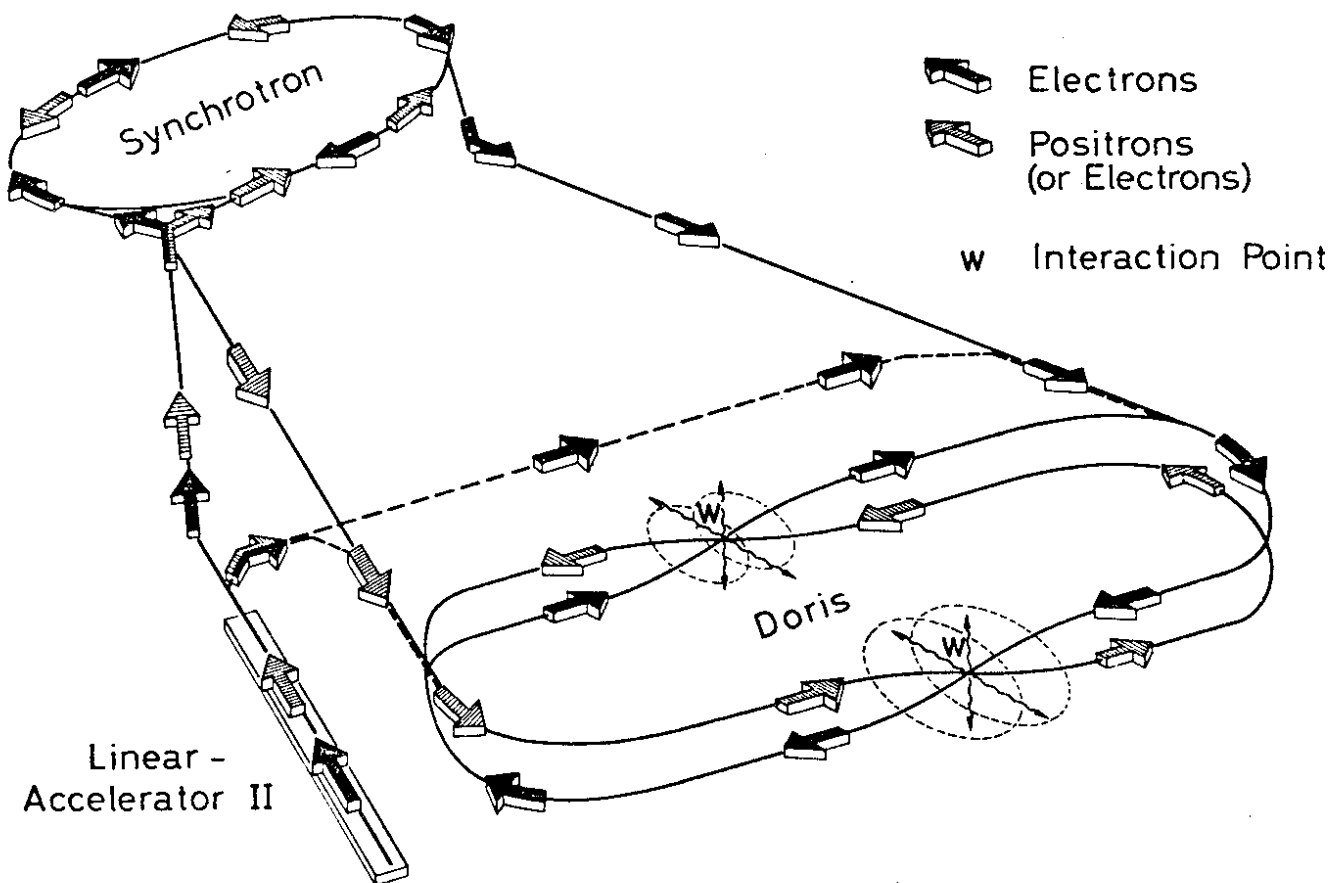
Fig. 1
Layout of the DESY accelerators

Although in principle CMS energies as high as 7 GeV can be reached with the present accelerator, all the data have been collected for energies between 3 GeV and 4.2 GeV. Upgrading the present magnet power supplies and installing all the available r.f. power in one ring will make it possible to reach a CMS energy of 10 GeV.

With the present optics the measured specific luminosity around 4 GeV (CMS) can be written as 10^{31} I^2 $(A^{-2}cm^{-2}sec^{-1})$ with the circulating current I measured in Amperes. This is in good agreement with the value of 1.2 I^2 10^{31} $(A^{-2}sec^{-1}cm^{-2})$ predicted from the present optics. So far luminosities in excess of 10^{30} $cm^{-2}sec^{-1})$ have been reached with stored currents of $0.3 - 0.4$ Ampere in each beam. However, at these high currents, the energy spread in the beam increases due to coherent synchrotron oscillations. These oscillations can be damped for currents less than $0.2 - 0.25$ Ampere by a second r.f. transmitter tuned slightly off the resonance frequency. Hence during the data taking at the 3.1 GeV and 3.7 GeV resonances, where a good mass resolution is imperative, the currents were limited to less than 0.25 Ampere. Another important parameter is

the size of the interaction volume. Due to the finite crossing angle and the high r.f. frequency used, the interaction "point" is around 2-3cm long. The transverse dimensions are less than 0.6 mm.

The main parameters of DORIS are summarized in Table I.

TABLE I:

Max.Energy:	7 GeV (9 GeV in the fall of 1975)
Average Circulating current:	0.200 - 0.400 Ampere / Ring
Number of Bunches:	1 - 480
Average Luminosity:	$\sim 3 \times 10^{29}$ $cm^2 sec^{-1}$
Beam lifetime:	> 6 hrs.
Gas pressure:	$1 - 5 \times 10^{-9}$ torr (depending on the current)
Interaction volume:	
along the beam	2 - 3 cm
transverse to the beam	< 0.6 mm.

DASP

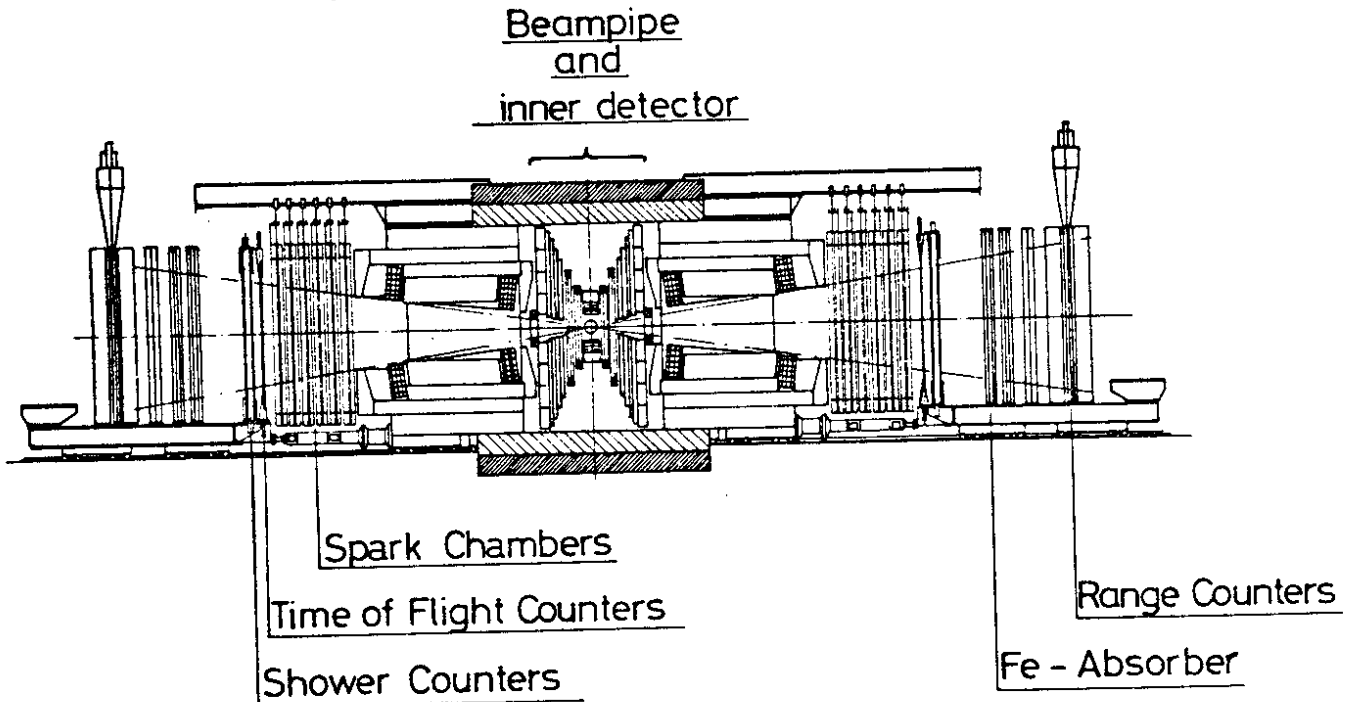A schematic drawing of DASP[4] viewed along the beam direction is shown in Fig. 2

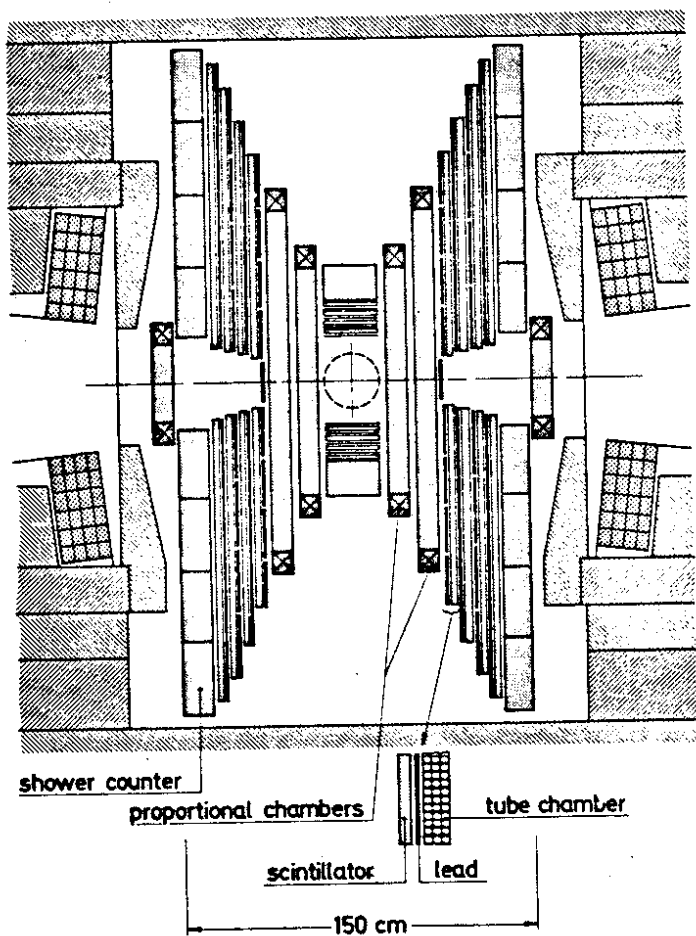Fig. 2 DASP viewed along the beam direction

Two large H-magnets are positioned symmetric with respect to the interaction point and spaced 2.1 m apart. The geometric acceptance of each magnet is from $48°$ to $132°$ in production angle and $\pm 9°$ in azimuth resulting in a solid angle of 2 x 0.45 sterad for both magnets. The acceptance for a charged particle is smaller than this and depends on the momentum, the field strength and last detector plane required. The maximum field strength is 1.1 Tesla, the integrated field length 1.8 Tm.

A charged particle emerging from the interaction point traverses the following detectors before reaching the magnet gap: a scintillation counter adjacent to the beam pipe, a second scintillation counter which starts the time of flight measurement, two proportional chambers (3 planes in each chamber, 2 mm wire spacing) a third scintillation counter used for triggering and a wire spark chamber with magnetostrictive readout (2 planes, 1 mm wire spacing).

The momentum of a charged particle is determined from the measurement of one space point on the trajectory in front of the magnet and the knowledge of the trajectory of the particle behind the magnet. The trajectory behind the magnet is measured by 6 wire spark chambers (each has 2 signal planes, 1 mm wire spacing, 5.6 by 1.7 m^2 sensitive area). At the present a resolution of $\pm 0.8\%$ is reached for a particle with 1.0 GeV/c momentum.

The particles are identified using time of flight, shower and range information:

The time of flight counters are mounted behind the spark chambers at an average distance of 4.7 m from the interaction point. The measured time of flight resolution is 0.5 nsec FWHM averaged over the 31 elements in one arm. This makes it feasible to separate pions and kaons for momenta less than 1.8 GeV/c, and kaons and protons for momenta less than 3 GeV/c, by time of flight alone. Hadrons and muons are separated from electrons by the pulse height in the shower counters. These counters are made of alternating sheets of lead and scintillator, a total of 6.2 radiation lengths thick. For an incident particle with a momentum of 1.5 GeV/c the cut in the shower pulse height can be made such that 80% of the pions but only 10^{-3} of the electrons have pulse heights below the cut, that is, an electron rejection in the pion signal of 10^{-3} in one arm. To further improve the electron-pion identification a fraction of the data was collected with a spark chamber positioned just after the shower counter.

The muons are positively identified by their range. The absorbers in the range telescope are made of iron a total of 90 cm thick, subdivided into plates of different thickness in order to allow for an optimal pion/muon separation at a chosen momentum. After each plate sufficient space for either a scintillation counter hodoscope or a spark chamber is provided. The main portion of the data were taken with one wall of scintillators at depth of 70 cm in the iron. This was later reduced to 60 cm and a spark chamber was installed at a depth of 40 cm in the iron.

The inner detector shown in Fig. 3 is located in the free space between the magnets. It is made out of proportional chambers, scintillation counters, proportional tube chambers, and shower counters. This part of the detector covers more than 70% of 4π and is well suited for a measurement of the direction and energy of photons and also the direction and, in some cases, the energy of charged particles.

The basic unit of the inner detector is a scintillation counter hodoscope, a sheet of lead 5 mm thick and a proportional tube chamber. The tube chambers consist of three (two) signal planes

shower counter
proportional chambers
tube chamber
scintillator
lead
150 cm

DASP — Inner Detector

Fig. 3
The inner detector of DASP
viewed along the beam direction

and measure the position to $\pm$ 5 mm ($\pm$ 7.5 mm). A particle emitted in the direction of the inner detector first traverses one of the 22 scintillation counters surrounding the beam pipe, the proportional chambers (in a part of the azimuthal acceptance), then four of the units just described, and finally a lead-scintillator shower counter eight radiation lengths thick. The direction of a shower is determined to about $\pm$ 2°, the energy resolution is around 30% for an incident photon of 1 GeV. The detector has a 50% efficiency for detecting a 50 MeV photon.

PLUTO

The DESY 4π detector PLUTO[5] is shown in Fig. 4 viewed along the beam direction. The main component of the detector is a superconducting solenoid
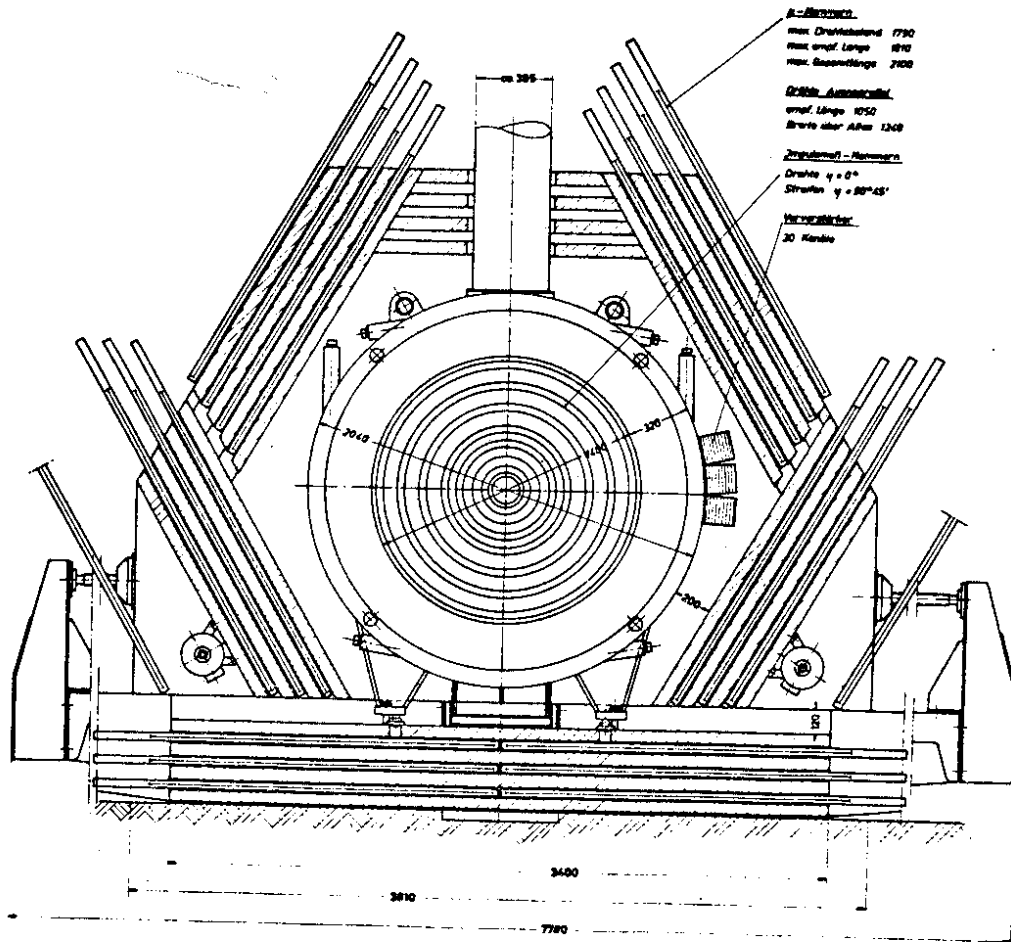

Fig. 4
PLUTO viewed along the beam direction

1.15 m long and 1.4 m in diameter. The magnetic field is parallel to the
beam axis; the maximum field strength is 2 Tesla. The solenoid is filled
with cylindrical multiwire proportional chambers with wires parallel
to the beam axis. The high voltage electrodes are also read out. They are
made of strips 16 mm wide, with dip angles of 45° with respect to the sig-
nal wires. The chambers cover a solid angle of 85% of 4π. To detect pho-
tons a cylindrical lead converter 0.41 of a radiation length thick is in-
serted at a radius of 39 cm. In the iron return yoke of the solenoid two
layers of proportional tube chambers for muon identification are inserted.
These chambers cover the full azimuthal angle for production angles between
73° and 107°. A second set of chambers close to the forward and backward
directions mounted on the outside of the iron yoke (50 cm thick) covers an
additional solid angle of 0.06 of 4π.

The fast signals from the proportional chambers are fed to a hard wired data-
processor, which reconstructs the track emerging from the interaction point.
This makes it feasible to trigger the system on well defined charged tracks
and reject beam-gas and cosmic ray events on line.

THE RESULTS

Inclusive spectra, particle ratios and mass searches

To measure the inclusive spectra the spectrometer was triggered on a single
charged particle traversing one of the arms of the spectrometer. The
trigger efficiency is thus independent of the final state and does not
introduce any systematic uncertainties between pions, kaons and protons.
Hadrons are separated from electrons and muons by the information from the
shower counters and the range counters as discussed above. Pions, kaons
and protons are identified by the time of flight information shown in Fig.5,
where $(1/\beta^2 - 1)$ as measured by the time of flight system is plotted ver-
sus $1/p^2$ at a CMS energy of 3.1 GeV. Since $(1/\beta^2 - 1) = M^2/p^2$ particles
of mass M will fall along a straight line, the locations predicted for pions,
kaons and protons are represented by the solid lines. The measured events
cluster along these lines and the plot shows that pions, kaons and protons
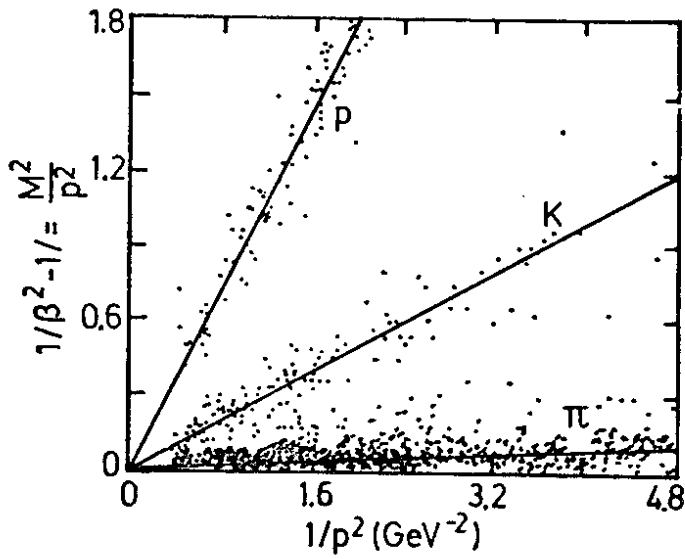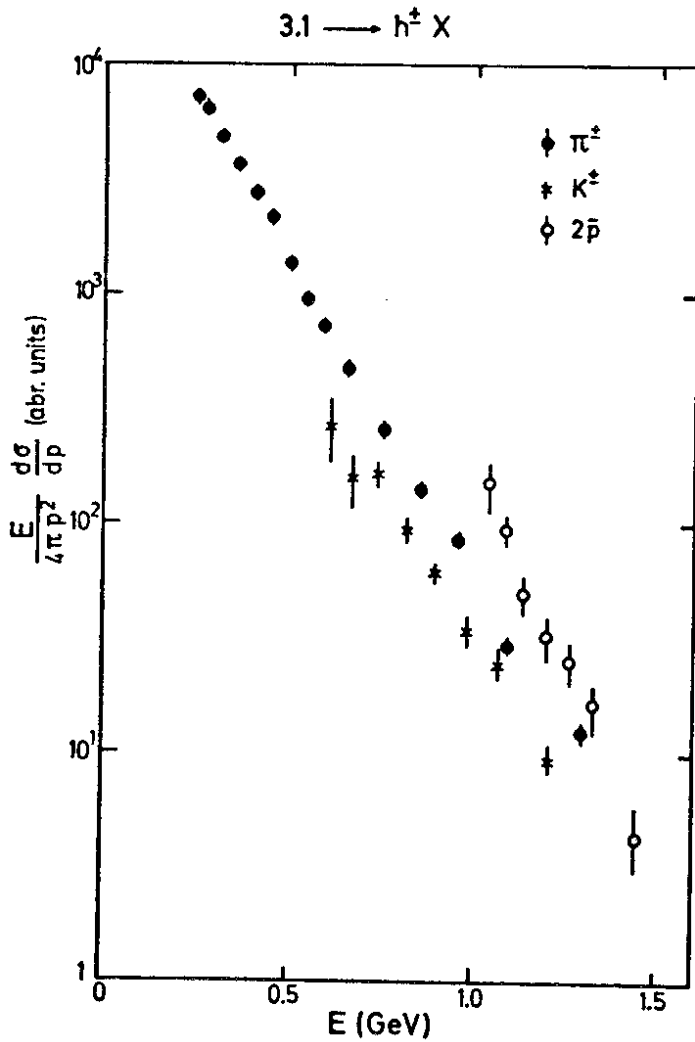are well separated at all momenta up to the kinematical boundary.

Fig. 5
Time of flight spectrum
measured at
$2E_{CM} = 3.1$ GeV

In Fig. 6 the invariant
cross section for the de-
cay $J/\psi \to h^{\pm}X^{\mp}$ is plotted
in arbitrary units versus
the particle energy for
pions, kaons and antipro-
tons (x2). The invariant
cross section for antipro-
tons seems to be larger
than the cross section for
pions and kaons. However,
note that the cross sec-
tions are roughly all the
same within a factor

Fig. 6
The invariant cross
section versus the par-
ticle energy for the
decay $J/\psi \to h^{\pm}X^{\mp}$

of three and tend to approach each other with increasing particle energy. To a good approximation, the invariant cross sections are decreasing exponentially with the particle energy E. For pions the energy dependence is well reproduced by e^{-6E}.

In Fig. 7 the invariant cross section for the decay $\psi' \to h^{\pm}X^{\pm}$ is plotted in arbitrary units versus the particle energy for pions, kaons and antiprotons (x2). The various cross sections show the same general behaviour as the cross se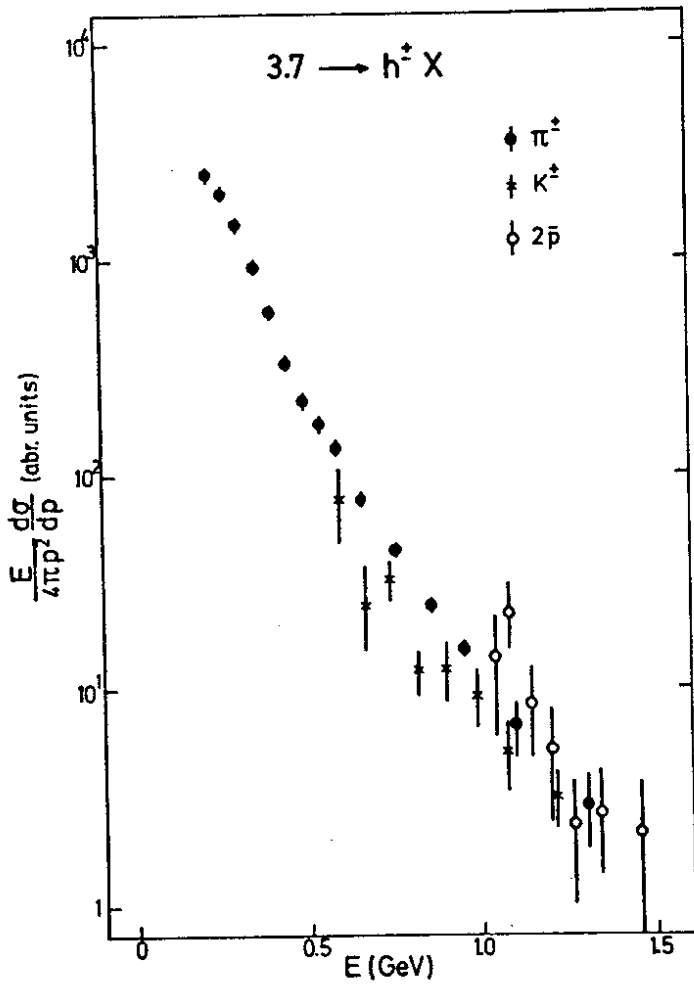ctions measured in the decay of the J/ψ resonance. This similarity might be expected, since the decay $\psi' \to J/\psi + X$ accounts[6] for roughly 60% of all the ψ' decays. The decay mode $\psi' \to \psi + \pi^+\pi^-$ is also seen directly as a step in the inclusive pion cross section at low pion energies.

Fig. 7
The invariant cross section versus
the particle energy for the decay
$\psi' \to h^{\pm}X$

The fraction of pions, kaons and antiprotons observed in the decay of the J/ψ and ψ' resonances is plotted in Fig. 8a, b as a function of momentum. Similar relative particle fractions are found at both resonances; at low momenta mostly pions are produced, but the relative yield of kaons and antiprotons increases with momentum. At a momentum of 1.0 GeV/c the relative fractions are 0.2 for kaons and 0.1 for antiprotons (x2). The data[7] obtained with the SPEAR solenoid on the particle fractions at the J/ψ resonance are also plotted in Fig. 8 a. The SPEAR results in general give a higher fraction of kaons and anti-protons.
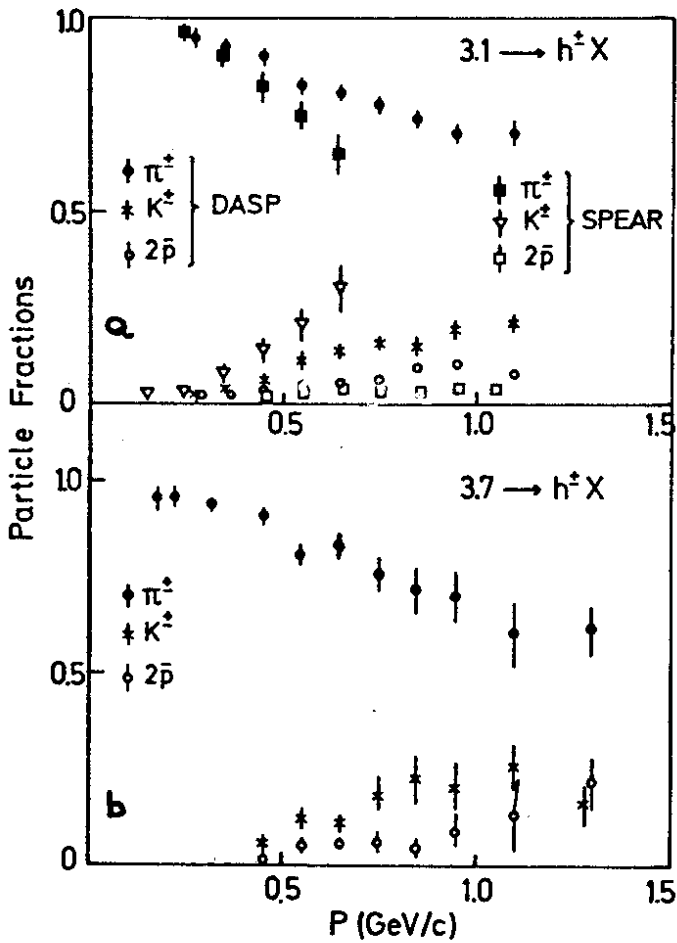

Fig. 8
Fractions of pions, kaons and antipro-tons (x2) observed
(a) at the J/ψ re-sonance and
(b) at the ψ' re-sonance

It has often been conjectured[8] that the relative yield of kaons might increase above 4 GeV due to the production and decay of charmed particles. No such increase was observed at a CMS energy of 4.15 GeV. This is seen in Table II where the relative particle fractions observed for momenta between 0.45 GeV/c and 1.3 GeV/c are listed and compared to the results obtained at the resonances.

TABLE II:

$2E_{CM}$	$\pi^{\pm}$/all	$K^{\pm}$/all	$2\bar{p}$/all
3.1	0.78 ± 0.008	0.14 ± 0.008	0.062 ± 0.006
3.7	0.82 ± 0.02	0.114 ± 0.013	0.065 ± 0.009
4.15	0.84 ± 0.09	0.10 ± 0.05	--
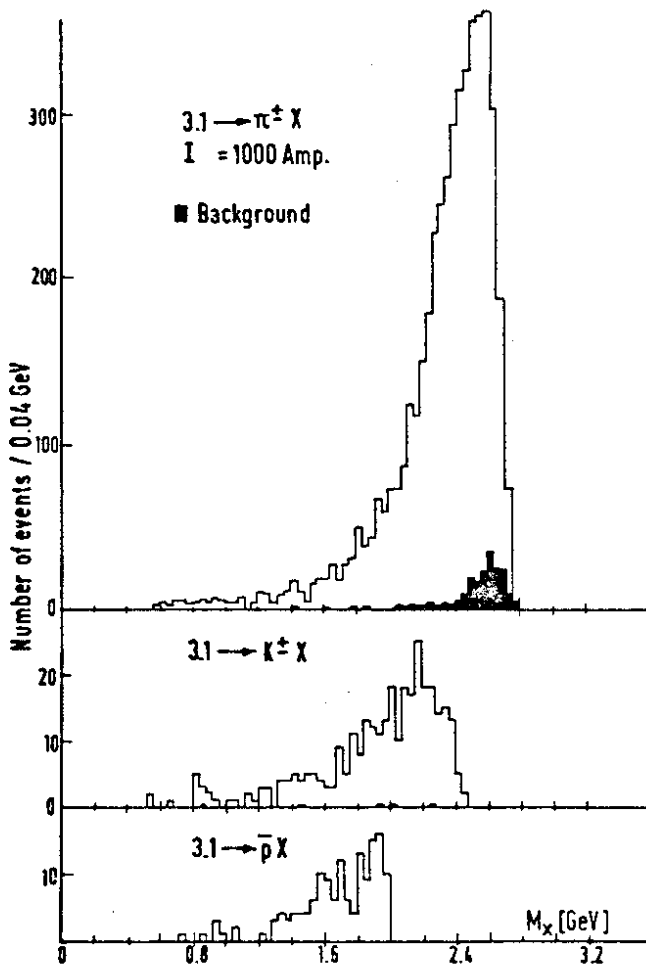
Any quasi-two body decay of the type $J/\psi(\psi') \to h + R$ will lead to a peak in the missing mass spectrum of states recoiling against the particle h. The missing mass spectra for the decay channels

$$J/\psi \to \begin{matrix} \pi^{\pm}X^{\mp} \\ K^{\pm}X^{\mp} \\ \bar{p}\ X^{+} \end{matrix}$$

are plotted in Fig. 9. Except for the existence of a possible $KK^{*}(890)$, no pronounced quasi-two body decays are observed. The background, shown as the black histogram in Fig. 9, was measured simultaneously with the data

Fig. 9
Missing Mass spectrum observed in the decay $J/\psi \to h^{\pm}X^{\mp}$

by selecting events originating outside of the interaction volume. The
estimated resolution in missing mass varied between 50 MeV and 10 MeV
for missing masses between the mass of the ρ and 2 GeV.

The missing mass spectra for the decay $\psi' \to h^{\pm}X^{\mp}$ are plotted in Fig. 10.
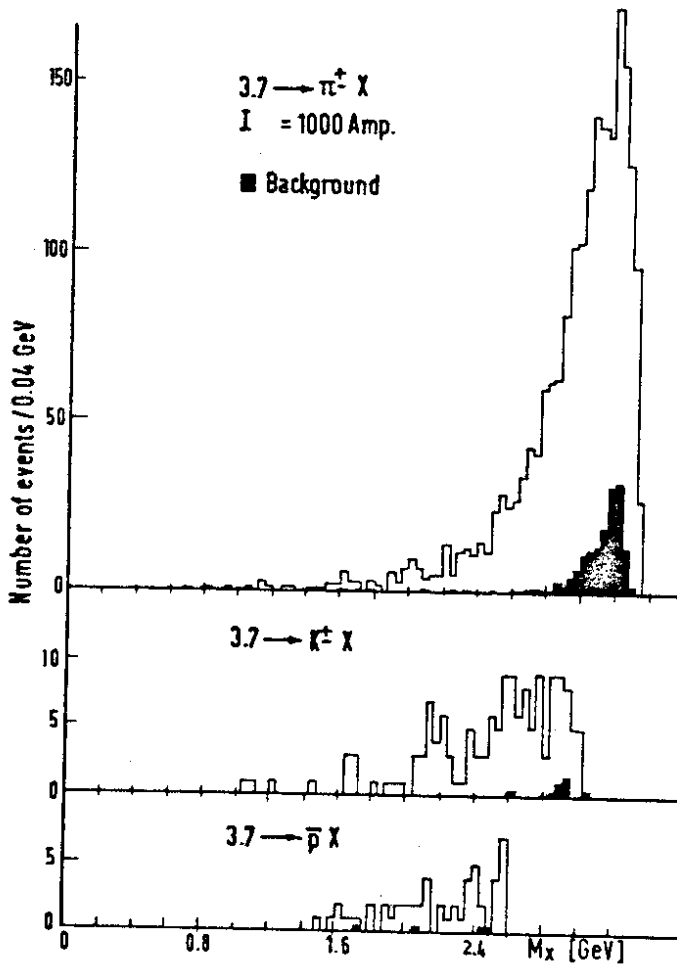No prominent structure with a confidence level of more than 4σ is observed.

According to the color[9]
interpretation of the new
resonances, the ψ' is expected to decay with the
emission of a single pion
into a colored meson ρ_c
with a mass around 3.1 GeV.
Therefore, if the ρ_c
exists, it will manifest
itself as a peak in the
missing mass spectrum observed in the decay
$\psi' \to \pi^{\pm}X^{\mp}$. To search for
this state a fraction of
the data was taken with
a reduced magnet current
to ensure a uniform mass
acceptance around 3.1 GeV.
There is no evidence for
such a peak in the measured
spectrum plotted in Fig. 10.
An upper limit on the decay $\psi' \to \pi^{\pm}\rho_c^{\mp}$ is derived
from these data assuming
the ρ_c to be less than
50 MeV wide. We find with

Fig. 10
Missing mass spectra measured
in the decays $\psi' \to h^{\pm}X$

90% confidence that

$$\frac{\Gamma_{\psi' \to \pi^{\pm} \rho_c^{\mp}}}{\Gamma_{\psi' \to \text{all}}} < 5 \times 10^{-2}.$$

$3.7 \longrightarrow \pi^{\pm} X$
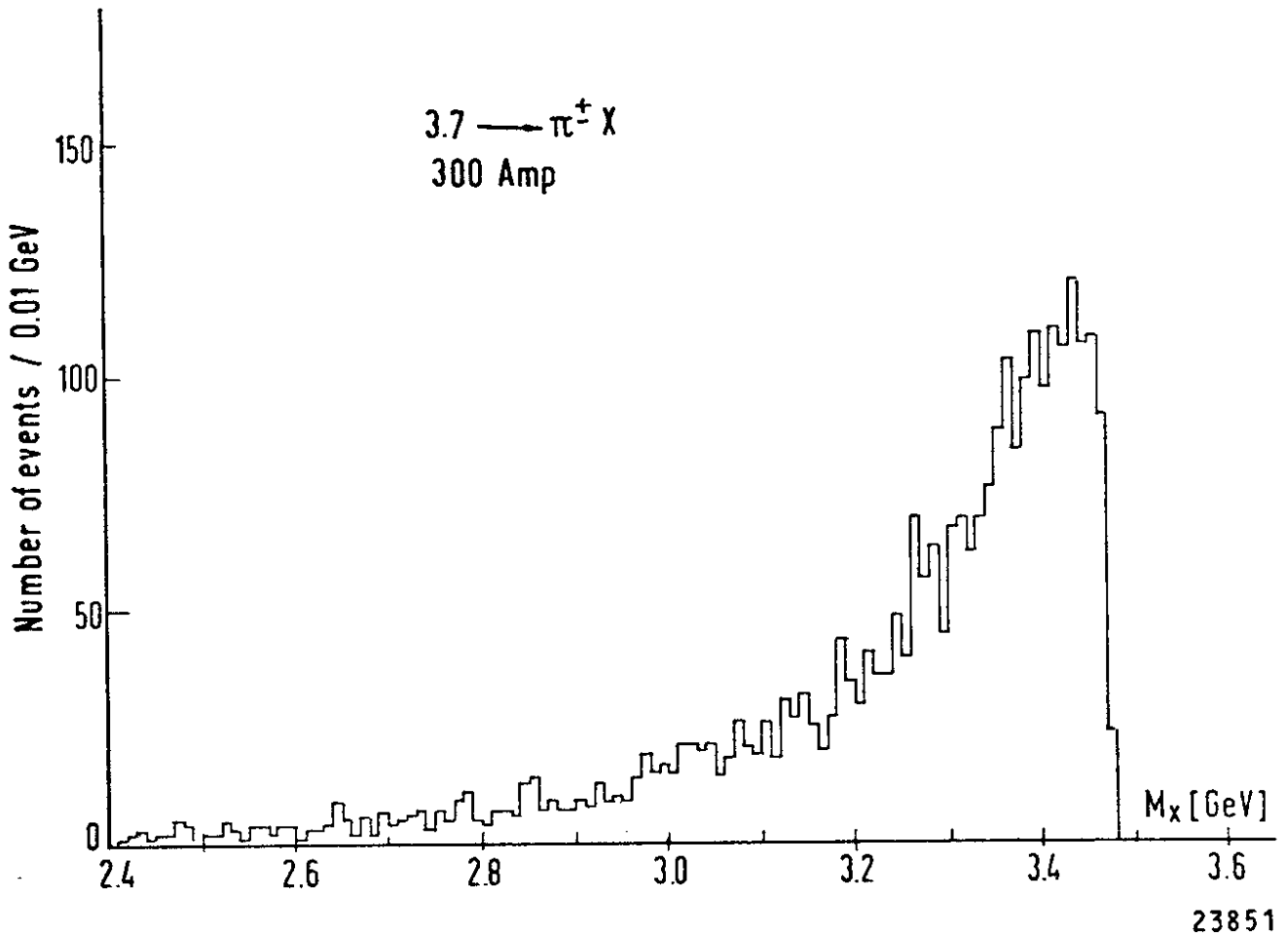
300 Amp

23851

Fig. 10
Search for $\psi' \to \pi^{\pm} \rho_c^{\mp}$ in the missing mass spectrum

HADRONIC TWO BODY DECAYS OF J/ψ and ψ'

The decay of the resonances into a pair of pions or kaons was searched
for by the DASP group[10] using the following criteria:

1) The two oppositely charged particles should be collinear to better
   than 0.15 rad and originate within the interaction volume.

2) The pair should have the correct momentum to within ± 50 MeV. The
   energy loss in the shower counter must be less than four times that

of a minimum ionizing particle and neither particle was permitted to fire the range counters.

At the J/ψ resonance no events, at the ψ' resonance one event satisfying the criteria above were found. The corresponding 90% upper confidence limits are listed in Table III. These limits were derived using the leptonic widths for the resonances measured[3] by the SPEAR solenoid group.

TABLE III:

Mode	J/ψ	ψ'
$\Gamma_{\pi^+\pi^-}/\Gamma$	$< 3 \times 10^{-4}$	$< 9 \times 10^{-4}$
$\Gamma_{K^+K^-}/\Gamma$	$< 6 \times 10^{-4}$	$< 1.6 \times 10^{-3}$

The absence of $\pi^+\pi^-$ events support the isospin and G-parity assignment $I^G = 0^-$. A small K^+K^- rate is expected if the new resonances are SU_3 singlet states.

The upper limits given on $\Gamma_{\pi^+\pi^-}/\Gamma$ and $\Gamma_{K^+K^-}/\Gamma$ for the J/ψ resonance are near the level where decay into $\pi^+\pi^-$ or K^+K^- pairs should occur via the second order radiative diagram. Extrapolating either the available data[11] or using the rho pole formula leads to $\Gamma_{\pi^+\pi^-}/\Gamma \sim 5\cdot10^{-4} - 5\cdot10^{-5}$ and a similar result for the K^+K^- decay.

The $p\bar{p}$ pairs were selected from the sample of pair events by demanding the correct time of flight. The effective mass spectrum of the $p\bar{p}$ pairs observed in the decay of the J/ψ resonance is plotted in Fig. 12. The elastic peak $J/\psi \to p\bar{p}$ is clearly seen centered at a mass of 3.09 GeV. To evaluate the branching ratio the angular distribution of the $p\bar{p}$ events must be known.

Assuming the angular distribution to be given by $1 + \cos^2\theta$ we find:
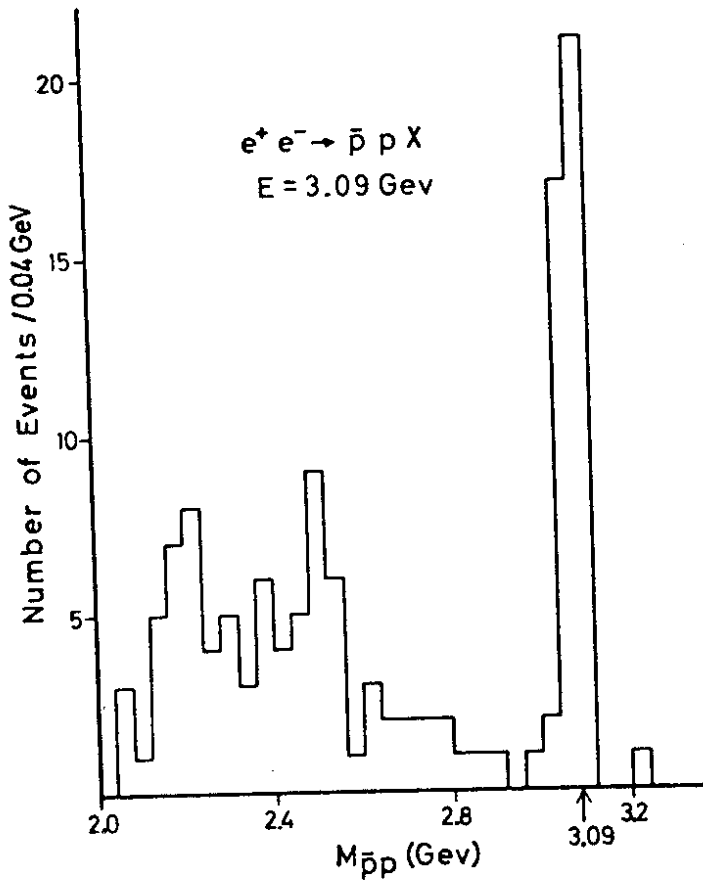
$$\Gamma_{p\bar{p}}/\Gamma = (0.0023 \pm 0.0006)$$

Fig. 12
Effective mass spectrum of
p̄p pairs from the decay of
the J/ψ resonance

This branching ratio was
derived using only a part
of the data plotted in
Fig. 12.
No candidates for the decay
ψ' → p̄p were found and the
upper limit is:

$$\Gamma_{p\bar{p}}/\Gamma \; < \; 0.001.$$

The decay J/ψ → p̄p has also
been measured with the
PLUTO detector. The hadron
pairs were selected from
a sample of collinear two
body events by demanding
the oppositely charged
particles neither to pene-
trate the muon shield nor to
produce a shower in the
lead absorber. It was further
required that the momentum
of the two particles should
balance to within 150 MeV.

Events satisfying these conditions are plotted in Fig. 13 as a function of 1/p. A cluster of events around $1/p = 0.812$ $(GeV/c)^{-1}$, the value expected for the decay $J/\psi \to p\bar{p}$, is observed. From these events, assuming a $(1 + \cos^2\theta)$ angular distribution, and the muon pair events measured in the same experiment the ratio

$$\Gamma_{p\bar{p}}/\Gamma_{\mu\mu} = 0.051 \pm 0.02$$

is determined directly.

I / P   DISTRIBUTION

$E_{BEAM} \approx 1.545$ GeV $B = 16$ KΓ

☐ ALL EVENTS

▨ SYMMETRIC EVENTS : $(P_+ - P_-) \leq .15\,GeV/c$
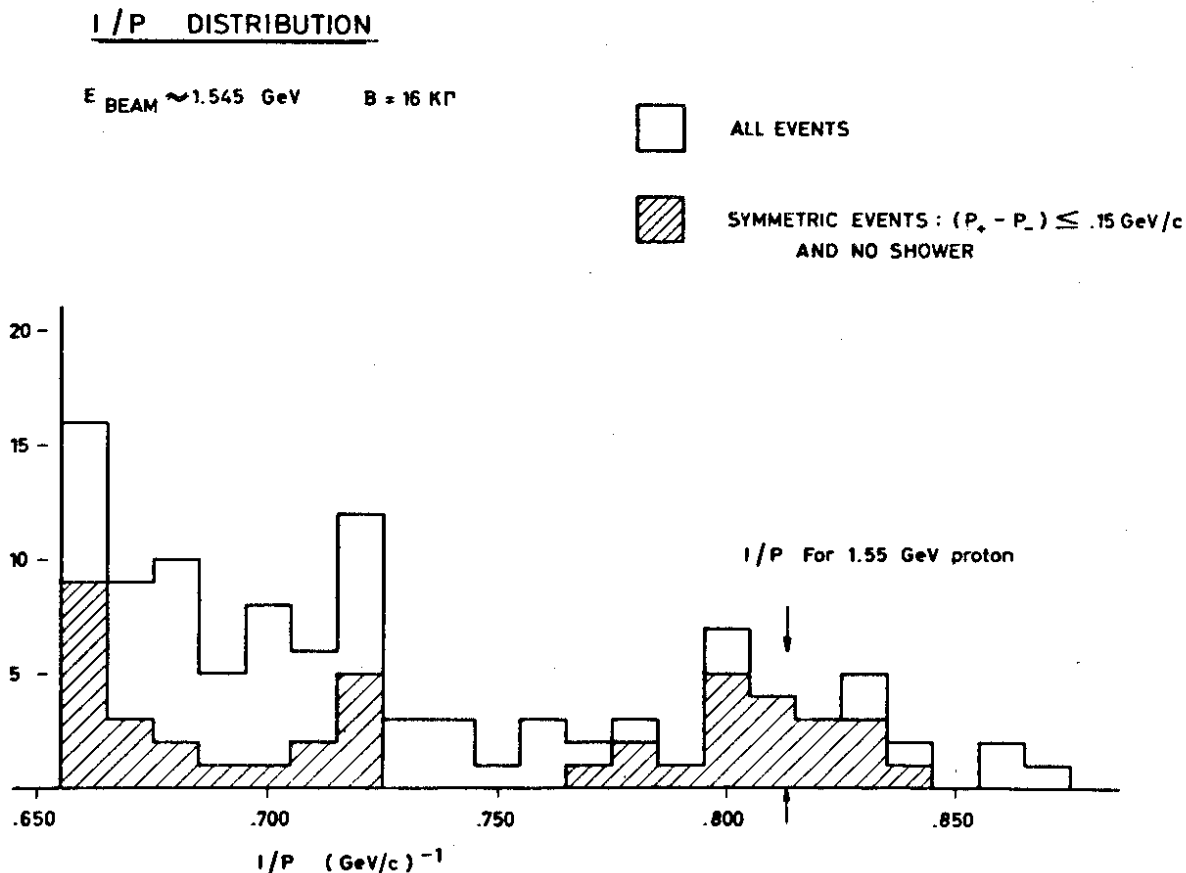AND NO SHOWER

I/P For 1.55 GeV proton

I/P $(GeV/c)^{-1}$

Fig. 13
The 1/p distribution for collinear pairs which
do not satisfy the criteria for muons or electrons.
Events with a large energy loss in one track are
excluded in the shaded histogram.

THE CASCADE DECAY: $\psi' \to J/\psi + X$

The yield of muon pairs produced at the ψ' resonance was measured by demanding one or both of two oppositely charged particles accepted by the magnets to penetrate 70 cm of iron. These criteria provide a clean sample of muon pairs; the contamination due to hadron pairs can be completely neglected. The effective mass spectrum plotted in Fig. 14 shows two peaks. The first peak is centered at the mass of the ψ' and is the sum of the decay of the ψ' into a pair of muons and the muons directly produced by QED. The second peak at a mass of 3.09 GeV is from the decay of the J/ψ resonance into a pair of muons and is direct evidence[6] for the decay $\psi' \to J/\psi + X$. The ψ' decays roughly 60% of the time via this channel.
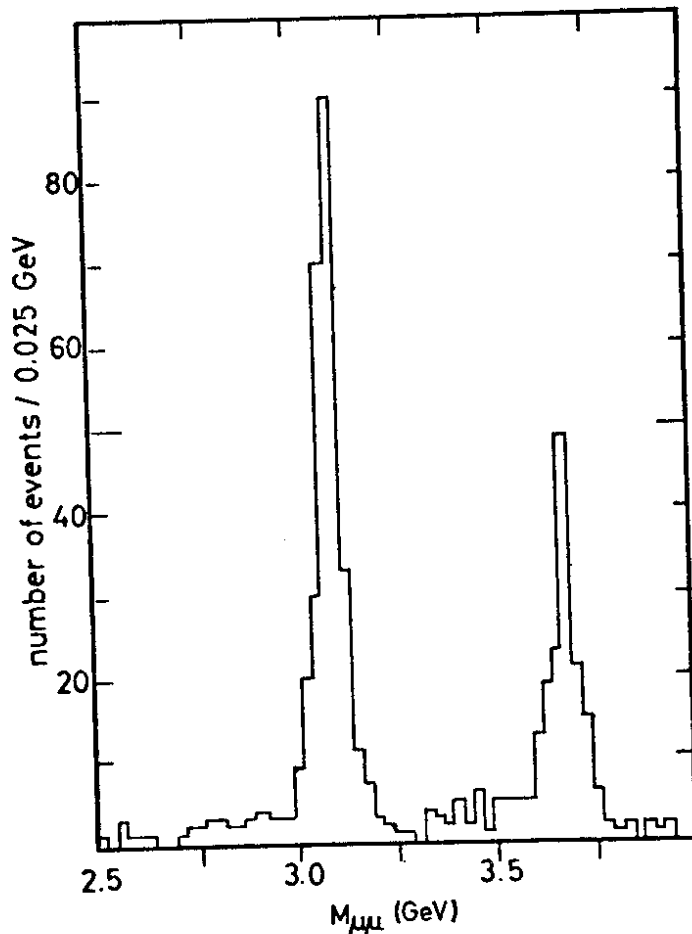

Fig. 14
The yield of muon pairs produced at the ψ'
resonance a function of the effective
pair mass

The following decay modes X are allowed by energy, charge and C-parity conservation:

$$\psi' \rightarrow (J/\psi) + \pi^0$$
$$\pi^+\pi^- \text{ or } \pi^0\pi^0$$
$$\pi^+\pi^-\pi^0 \text{ or } \pi^0\pi^0\pi^0$$
$$\eta$$
$$2\pi^+\pi^- \text{ or } 2\pi^0\pi^0$$
$$\gamma\gamma$$

The $\gamma\gamma$ mode can arise from two successive transitions through a new intermediate state P_c. Evidence for such states has now been obtained[12] and will be discussed below.
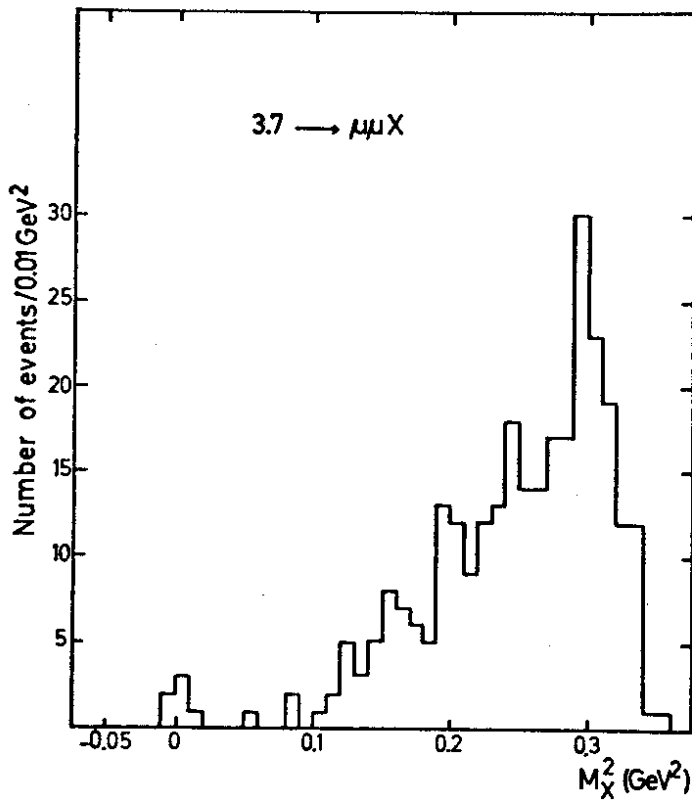

3.7 ⟶ $\mu\mu X$

Fig. 15
The spectrum of missing masses in the reaction $e^+e^- \rightarrow \mu^+\mu^- +$ missing mass produced at the ψ' resonance. The $\mu^+\mu^-$ effective mass is required to be between 2.9 GeV and 3.2 GeV

The cascade decays were investigated in more detail by selecting events with a muon pair mass between 2.9 GeV and 3.2 GeV. For these events, the missing mass recoiling against the $\mu^+\mu^-$ pair was computed from the known muon momenta assuming the pairs result from the decay of the J/ψ resonance. The spectrum, plotted in Fig. 15 as a function of missing mass shows a strong tendancy to peaks at high masses, with only a few events below the two pion threshold. In particular there is no evidence for decays with the emission of a single π^0.

The decay $\psi' \to J/\psi + \eta$ is observed in the missing mass spectrum as a narrow peak centered around 0.3 GeV^2. The observed width is consistent with the value expected from the experimental resolution alone. The existence of this decay mode proves that the ψ' and the J/ψ have the same isospin and G-parity.

The measured branching ratio

$$\frac{\psi' \to J/\psi + \eta}{\psi' \to \text{all}} = (0.037 \pm 0.015)$$

is surprisingly large considering the small phase space available.

The other decay modes listed above were disentangled using additional information from the inner detector. The results are:

1) No $2\pi^+\pi^-$ or $2\pi^0\pi^0$ events were found. The phase space available for these decay modes is exceedingly small.

2) Events with mixed charged and neutral tracks were found. These events are all consistent with either η decay or $\pi^0\pi^0$ decays with photons converting in the beam pipe. We have therefore no evidence for direct decays with the emission of $\pi^+\pi^-\pi^0$.

3) $\psi' \to J/\psi + \pi^+\pi^-$ is the dominant decay mode. The measured branching ratio is:

$$\frac{\psi' \to J/\psi + \pi^+\pi^-}{\psi' \to \text{all}} = 0.36 \pm 0.06$$

4) The decay $\psi' \to J/\psi + \pi^0\pi^0$ is directly observed with a branching ratio

$$\frac{\psi' \to J/\psi + \pi^0\pi^0}{\psi \to \text{all}} = 0.18 \pm 0.06$$

The measured ratio of $\pi^0\pi^0/\pi^+\pi^-$ is consistent with 0.5 as expected for a $\Delta I = 0$ transition. Pure $\Delta I = 1$ or 2 transitions corresponds to a ratio of 0 or 2 and this is excluded by the data.

EVIDENCE FOR NEW NARROW RESONANCES P$_c$

The decay mode $\psi' \to J/\psi + \gamma\gamma$ was found in two nearly independent experiments. In the first experiment the $\gamma\gamma$ cascade was identified by measuring the two electrons from the decay of the J/ψ resonance in coincidence with the photons. All four particles were observed in the inner detector

only. In a second experiment, done concurrently with the first, the reaction was identified by observing the decay of the J/ψ into a pair of muons with the magnetic spectrometer and selecting events with just two photons in the inner detector.

Since both experiments give the same absolute rate for the $\gamma\gamma$ transition, but the photon resolution obtained in the first experiment is not sufficient to separate the various transitions, only the second experiment will be discussed here.

The decay $\psi' \rightarrow (J/\psi \rightarrow \mu\mu) + \gamma\gamma$ was measured by first selecting those events which had a pair of muons accepted by the magnets in coincidence with two photons detected in the inner detector.

The muons were measured and identified as discussed above. The effective mass of the muon pair should be between 2.9 GeV and 3.2 GeV.

A photon in the inner detector was defined as follows:

The appropriate beam counters and front counters in the inner detector should not have fired. The photon should convert "in" the detector as evidenced by either a pulse in the shower counter (the energy loss must be greater than 0.3 of that for a minimum ionizing particle) or at least one proportional tube and one scintillation counter fired. The angular resolution for photons is $\pm 2^{O}$ if they convert in front of a proportional tube chamber or $\pm 8^{O}$ in ϕ and $\pm 20^{O}$ in θ if they are detected by the shower counters only.

Altogether 33 events that satified these criteria were found. Besides the genuine $\gamma\gamma$ events this sample also contains background events resulting from the decays:

$$\psi' \rightarrow (J/\psi \rightarrow \mu\mu) + \eta$$
$$\rightarrow (J/\psi \rightarrow \mu\mu) + \pi^{o}\pi^{o}$$

where two of the photons produced are detected.

The η background was removed by restricting the missing mass recoiling against the $\mu^{+}\mu^{-}$ pair to values less than 520 MeV. To remove the $\pi^{o}\pi^{o}$ contribution, a 3C fit to the remaining sample of 29 events was made assuming these events to be genuine $\gamma\gamma$ events. The measured momenta and

angles of the muons and the direction of the photons were used as an input to the computation together with their errors. The events were then plotted as a function of the chi square of the fit. Candidates for genuine $\gamma\gamma$ events were required to have a χ^2 of less than 12. Altogether 9 events satisfied these criteria. The $\pi^0\pi^0$ background remaining in this sample was evaluated by a Monte Carlo calculation, using as input:

1) (The $\pi^0\pi^0$ mass spectrum) = 1/2 (the $\pi^+\pi^-$ mass spectrum observed in $\psi' \to J/\psi + \pi^+\pi^-$). This relationship is found experimentally and is predicted for a $\Delta I = 0$ transition.

2) The acceptance of the detector computed from the known geometric acceptance and the measured detection efficiency for a photon.

The Monte Carlo computation predicted that of the remaining 9 events less than 0.8 event results from $\pi^0\pi^0$ decays.
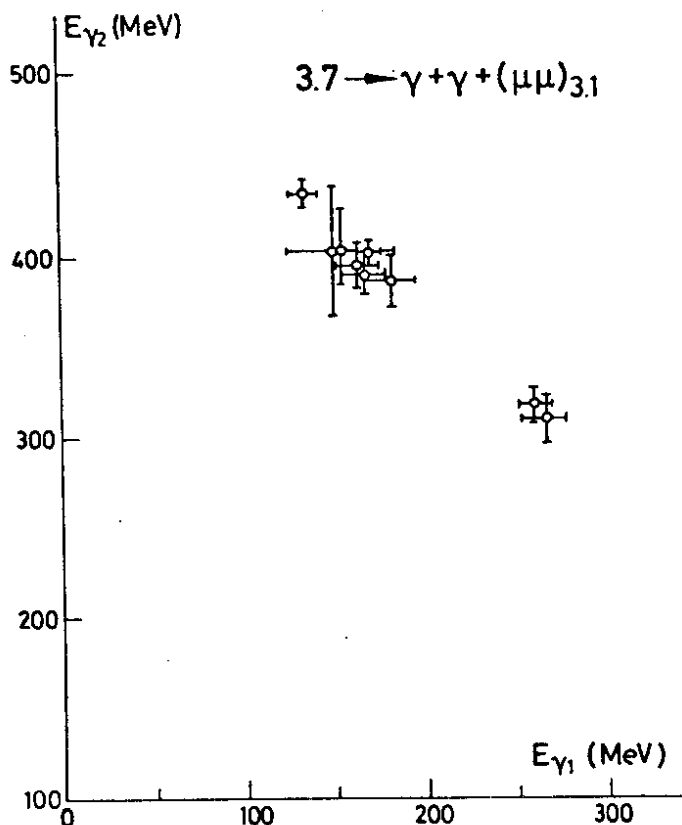

Fig. 16
Scatter plot of the two photon energies for candidates for the decay $\psi' \to (J/\psi \to \mu^+\mu^-) + \gamma\gamma$

The events are plotted in Fig. 16 as a function of the fitted photon energies. The events cluster in two groups demonstrating the existence of two narrow resonances P_c and P'_c with even charge conjugation.

The first group is centered at:

$E_{\gamma 1} = (169 \pm 7)$ MeV

$E_{\gamma 2} = (398 \pm 7)$ MeV.

It can not yet be decided in which order these photons are emitted and this leads to a twofold ambiguity in the mass of the new particle

$$M_{P_c} = (3.507 \pm 0.007) \text{ GeV}$$

$$\text{or} \quad M_{P_c} = (3.258 \pm 0.007) \text{ GeV}.$$

It seems, however, natural to associate the P_c resonance with the resonance later observed at (3.53 ± 0.02) GeV by the SPEAR group[13].

The total branching ratio:

$$\frac{\psi' \to P_c + \gamma_1}{\psi' \to \text{all}} \cdot \frac{P_c \to J/\psi + \gamma_2}{P_c \to \text{all}} = (0.04 \pm 0.02)$$

A second group, consisting of two events, is centered at:

$$E_1 = (263 \pm 8) \text{ MeV}$$

$$E_2 = (315 \pm 8) \text{ MeV}$$

This corresponds to a mass of:

$$M_{P'_c} = (3.407 \pm 0.008) \text{ GeV}$$

$$M_{P'_c} = (3.351 \pm 0.008) \text{ GeV}$$

It might be tempting to associate this state with χ (3.41 ± 0.01) GeV found[13] by the SPEAR group.

States with even charge conjugation were predicted[14] by the charm model to exist in the mass range between 3.7 GeV and 3.1 GeV. The various charmonium models further predict these states to decay with a large branching ratio into the J/ψ resonance plus a photon. From a comparison of the branching ratio measured for the $\gamma\gamma$ cascade in this experiment and the limits obtained[15] on a single mono energetic photon line in the decays of the ψ' resonance, one concludes that $P_c \to J/\psi + \gamma$ must indeed be a major decay mode of the new resonance.

It is therefore tempting to associate the new P_c resonances with the states predicted in the charmonium model. However, one should bear in mind that since these states might also be accomodated in a color model[9], their mere existence proves neither charm nor color.

If the P_c is a natural spin parity state it can decay into a pair of pseudoscalar mesons. The decay $\psi' \rightarrow (P_c \rightarrow \pi^+\pi^-, K^+K^-) + \gamma$ has been searched for by observing pairs of pions (kaons) with the magnetic spectrometers of DASP in coincidence with a photon in the inner detector. Two candidates for this decay are found, one at an invariant pair mass of 3.515 GeV, the other at a mass of 3.439 GeV. Each event represents a branching ratio:

$$\frac{\psi' \rightarrow P_c \cdot \gamma}{\psi' \rightarrow all} \quad . \quad \frac{P_c \rightarrow \pi^+\pi^-, K^+K^-}{P_c \rightarrow all}$$

of the order of 2×10^{-4}.

The SPEAR solenoid group found[13] the $\chi(3410)$ to decay into pion plus kaon pairs with a branching ratio, as defined above of $(13 \pm 5) \cdot 10^{-4}$. They found no candidates at the mass of the P_c resonance; their 90% confidence upper limit was 2.7×10^{-4}.

THE TWO PHOTON FINAL STATE

The cross section for two collinear or nearly collinear photons has been measured[16] by demanding a coincidence between the sectors of the inner detector mounted above and below the beam pipe. Bhabha scatters and cosmic ray events were rejected by requiring that no more than two of the two upper and two lower layers of scintillators between the interaction point and the first lead converters be fired. This allows for the possibility that one of the two photons converts in the beam pipe. The remaining background from beam-gas interactions and cosmic ray events was removed by cuts in the energy deposited, number of proportional tubes fired and the time of flight.

Collinear photon pairs are produced in the two photon annihilation $e^+e^- \rightarrow \gamma\gamma$. Superimposed on this smoothly decreasing cross section there might be a peak at the mass of the resonances due to any of the following processes:

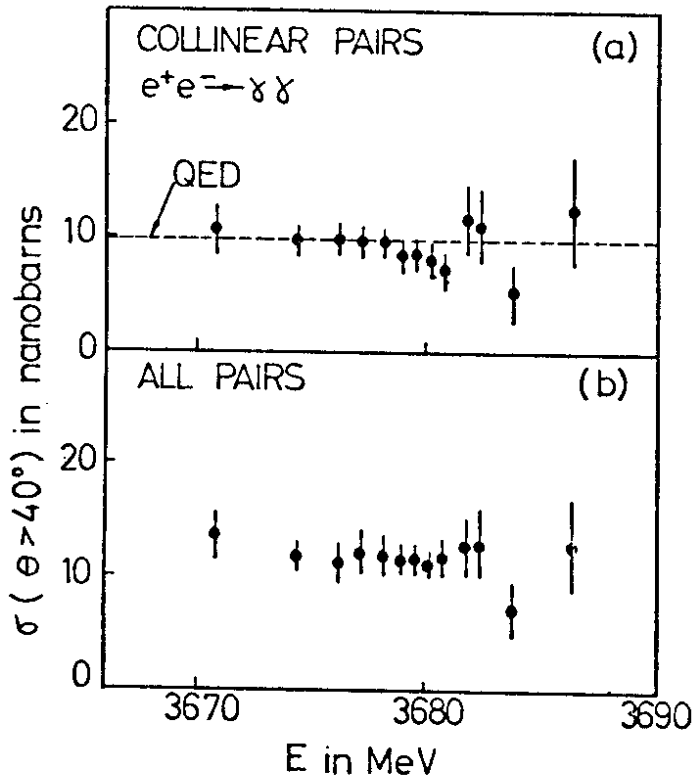1) Direct decay of the resonances into a pair of collinear photons. This

decay is strictly forbidden for a spin 1 state. It is allowed for all other values of the spin provided C is even or not conserved.

2) $e^+e^- \to \psi/J~(\psi') \to \pi^0 + \gamma$. In this case there will always be two photons non collinear to within an angle of m_π/E_π. If the second photon from the π^0 decay is not detected the event will masquerade as a $\gamma\gamma$ event.

3) $e^+e^- \to \psi/J~(\psi') \to (X \to \gamma\gamma) + \gamma$

The resonance decays with the emission of a single photon into a heavy particle X which in turn decays into two photons. If the mass of X is close to 3.1 GeV or 3.7 GeV, X will be produced nearly at rest and the two photons from its decay will be nearly collinear.

The measured energy dependence of the $\gamma\gamma$ cross section is plotted in Fig. 17 and Fig. 18 for energies in the vicinity of 3.09 GeV and 3.68 GeV. No resonance effect is observed and the absolute value of the cross section is in good agreement with the predicted QED cross section shown as the dotted line.

Fig. 17
Cross section for $e^+e^- \to \gamma\gamma$ as a function of CMS energy in the vicinity of 3.09 GeV. The dotted line is the rate predicted from QED
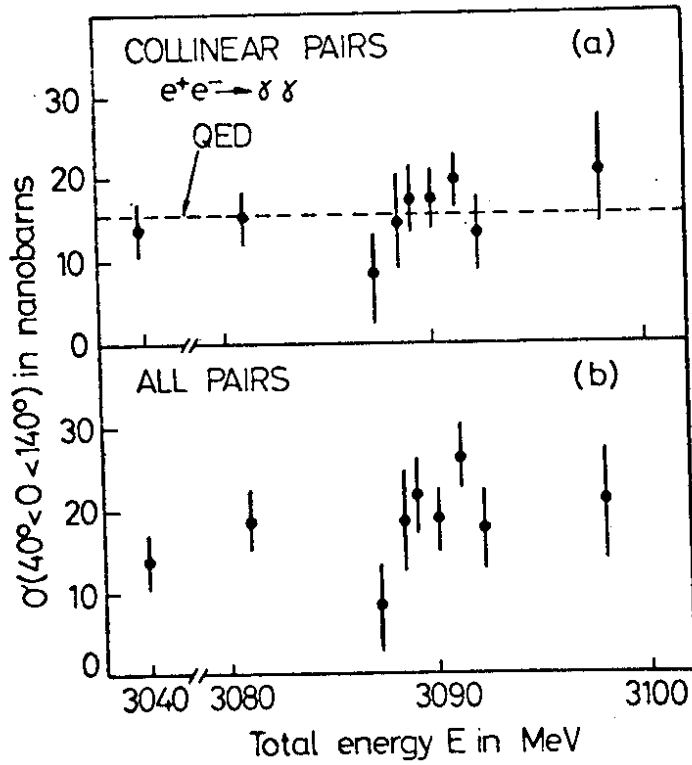
Fig. 18
Cross section for $e^+e^- \rightarrow \gamma\gamma$
as a function of CMS energy
in the vicinity of 3.68 GeV.
The dotted line is the rate
predicted from QED

The angular distributions, plotted in Fig. 19a, b are also consistent with
QED predictions, plotted as the dashed line. Upper limits on the various
resonance contributions were derived from the observed energy dependence
of the cross sections by fitting the data to a nonresonant background
plus a Gaussian peak with the mass and the width observed in the total
hadron cross section using the same detector. The 90% confidence upper
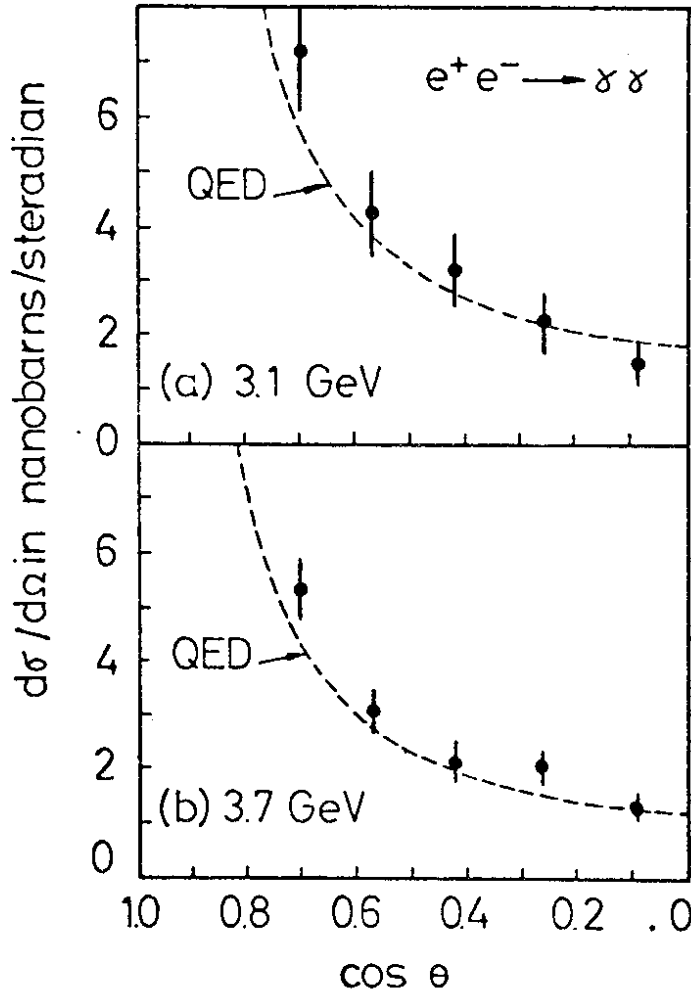limits are listed in Table IV:

Fig. 19
Angular distributions
of $e^+e^- \to \gamma\gamma$

a) for CMS energies
   near 3.09 GeV

b) for CMS energies
   near 3.68 GeV

The dashed lines are the
angular distributions pre-
dicted from QED

TABLE IV:

Mode	J/ψ	ψ'
$\Gamma_{\gamma\gamma}/\Gamma$	0.003	0.008
$\Gamma_{\pi\gamma}/\Gamma$	0.01	0.01
$(\Gamma_{X\gamma}/\Gamma)(\Gamma_{X\to\gamma\gamma}/\Gamma_{X\to all})$	0.003 (2.99GeV<M_x<3.09GeV)	0.008 (3.58GeV<M_x<3.68GeV)

THREE PHOTON FINAL STATE AND EVIDENCE FOR A NEW RESONANCE

The production of three photons in e^+e^- annihilation at CMS energies around 3.09 GeV and 3.68 GeV has been measured with the DASP inner detector. The following processes might contribute to the observed yield:

1) Quasi two body decays:

$$J/\psi\ (\psi') \rightarrow (X \rightarrow \gamma\gamma) + \gamma$$

The $\eta\gamma$ and $\eta'\gamma$ decay modes of the resonances have been identified, but the analysis of the $\pi^0\gamma$ mode is not yet complete. There is also evidence for a new resonance X decaying into two photons at a mass around 2.75 - 2.8 GeV.

2) Direct decay of the resonances into three photons. An evaluation[17] of this shows that no peaks appear in the effective mass spectrum for any combinations of two photons.
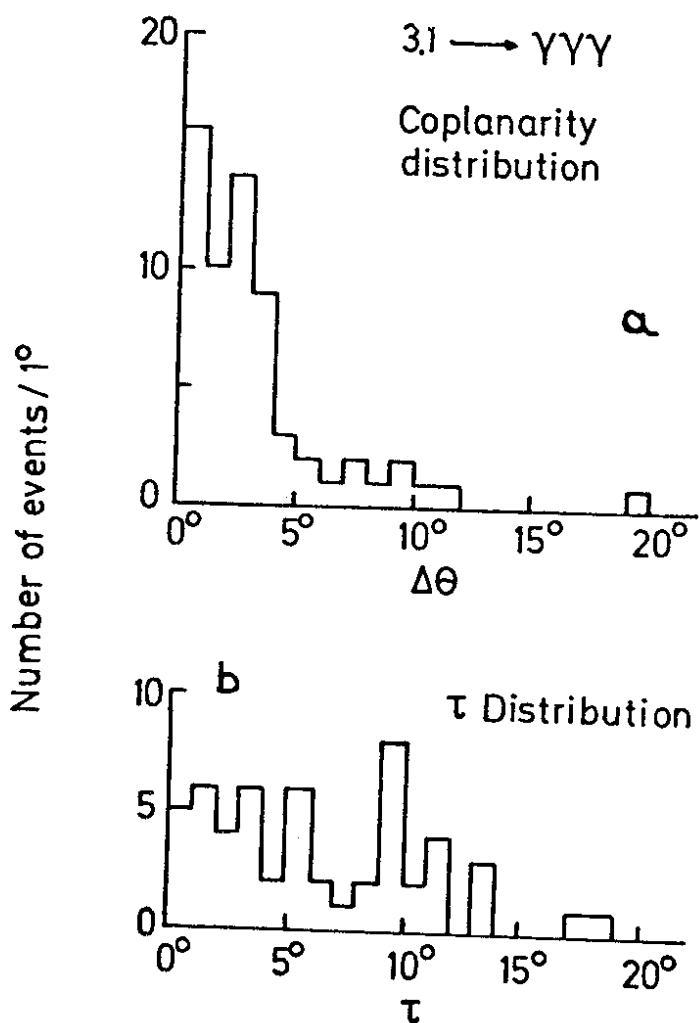
3) Direct production of a three photon final state via the QED diagrams. This is the most serious background encountered in the three photon channel and will be discussed below.

The three photon final states were selected using the following criteria:

1) Only three photons should be observed in the final state. Events with photons converting in the beam pipe were rejected.

2) The opening angle of any pair of photons should be greater than 30°. This removed any $\pi^0\gamma$ events.

Demanding a three photon final state effectively removed the background resulting from beam-gas interactions, cosmic ray events and multihadron events. This is seen in Fig. 20a where the events produced at a CMS energy of 3.09 GeV are plotted versus a coplanarity "angle" $\Delta\theta$. $\Delta\theta$ is defined as the invariant quantity arc $\sin((\vec{n}_1 \times \vec{n}_2) \cdot \vec{n}_3)$ where $\vec{n}_j$ is the unit vector along the direction of the photon j. The distribution peaks at small values of $\Delta\theta$ as expected for genuine three photon events, and the observed width is consistent with the width expected from the experimental resolution. Events with $\Delta\theta > 5^\circ$ were rejected. Of the

68 events contained in the plot 52 events survived the cut.

Fig. 20
a) Number of three photon events versus the coplanarity angle $\Delta\theta$
b) Number of three photon events with $\Delta\theta < 5°$ versus to the angle τ (defined in the text)

The fraction of QED events in the remaining sample was reduced by excluding events with the beam axis in (or close to) the event plane. This cut was made by projecting the unit vectors $\vec{n}_j$ onto a plane normal to the beam axis and defining the smallest non collinearity angle τ between any of two projected vectors. QED events peak at small values of τ; the other events do not. Events with $\tau < 5°$ are rejected.

The remaining events and the total integrated luminosity are listed in Table V.

TABLE V:

$2E_{CMS}$	J/ψ	ψ'	Outside the resonances
Number of events	30	15	4
Integrated luminosity	211 nb^{-1}	367 nb^{-1}	118 nb^{-1}

The photon energies were computed from the measured directions of the photon and the known CMS energy assuming the remaining events to be genuine three photon events. The effective mass between any two photons in the event was computed from the measured opening angle and the derived photon energy. The mass resolution $\Delta M/M$ estimated at a CMS energy of 3.1 GeV varied between $\pm 5 \times 10^{-2}$ and $\pm 1.5 \times 10^{-2}$ for values of M between 0.5 GeV and 2.8 GeV.
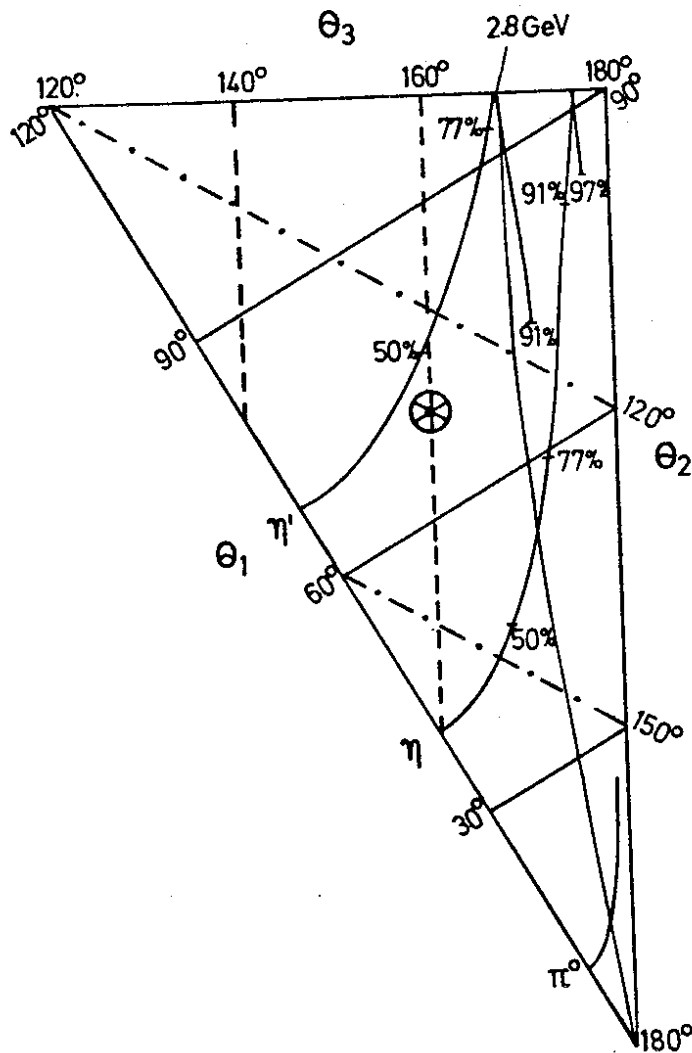
The events were plotted as a function of the largest and the smallest opening angles θ_3 and θ_1 occurring between any two photons in the event. This plot, compared to a Dalitz plot, has the advantage that the measured photon direction is plotted directly so that the errors involved are constant everywhere in the plot. The main features of the plot are demonstrated in Fig. 21 for a CMS energy of 3.1 GeV.

Fig. 21
Plot of an event as a function of the smallest and the largest opening angles θ_1 and θ_3 occurring in the event.

All the events are mapped within the triangle as a function of θ_1 and θ_3. The smallest opening angle θ_1 varies between $0°$ and $120°$ and is constant along lines normal to the hypotenuse of the triangle. The largest opening angle θ_3 varies between $120°$ and $180°$ and is constant along the dotted lines. The third opening angle θ_2 varies between $90°$ and $180°$ and is the difference between $360°$ and the sum θ_1 plus θ_3. It is constant along the point-dotted lines. The errors involved are indicated by the size of the symbol plotted.
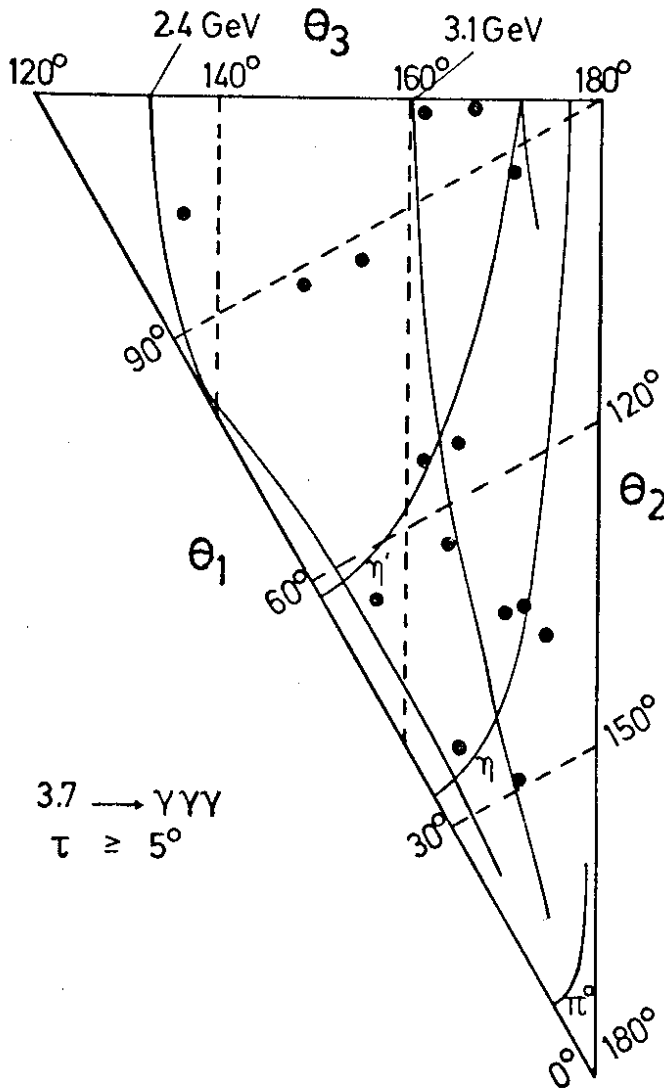

Fig. 22
Plot of the three photon events obtained at the ψ' resonance

Lines of constant effective mass are drawn for the mass of the η, the η' and a hypotetical heavy particle of 2.8 GeV. The distribution of the events along these curves are also indicated. The η and the η' are peaked at small angles, the heavy particles are roughly uniformly distributed along the curve.

The events measured at a CMS energy of 3.68 GeV and 3.09 GeV are plotted in Fig. 22 and Fig. 23 as a function of the opening angles θ_1 and θ_3. The events observed at the ψ' resonance do not cluster along any particular mass value in contrast to the events measured at the J/ψ resonance. Here a clear clustering of events

is observed along the curves representing the mass of the η and that of a hypotetical heavy particle of mass around 2.8 GeV. The events are plotted as a function of the lowest and the highest effective mass found in each event in Fig. 24 for the ψ' resonance and in Fig. 25 for the J/ψ resonance. In the high mass plot at 3.1 GeV all events which had one of the two remaining effective mass values within $\pm$ σ of the mass of an η or an η' are removed from the plot.

At the mass of the ψ' the events are essentially uniformly distributed as a function of the low mass solution with neither a clear η nor a η' signal. Also in the high mass solution no significant peaking is observed. The events tend to have
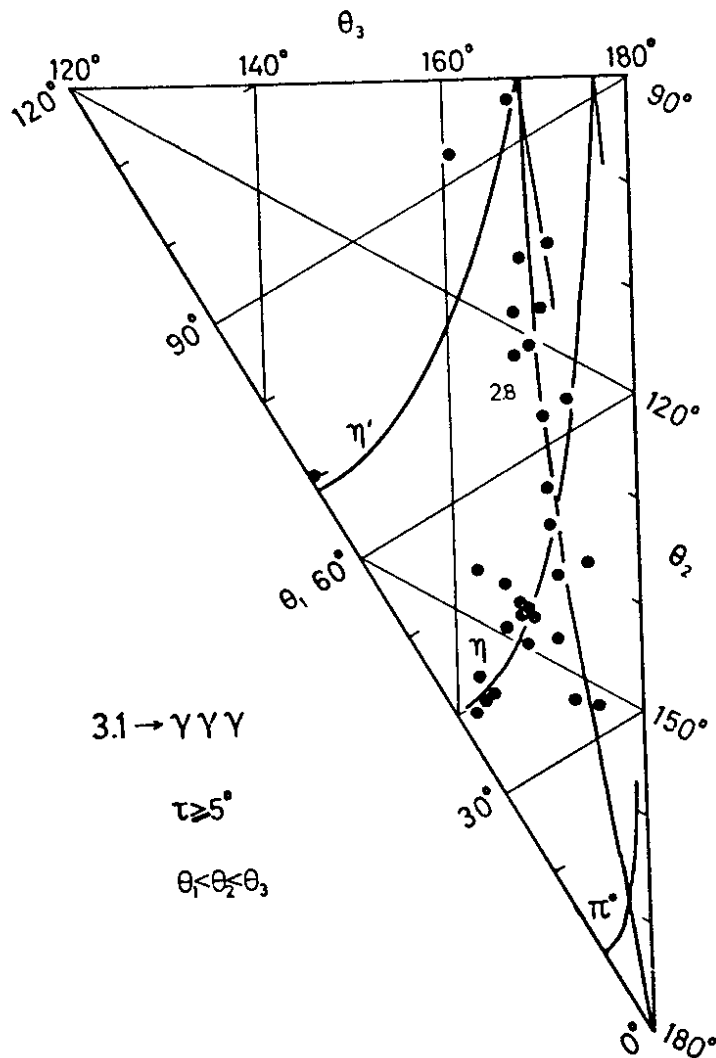

Fig. 23
Plot of the three photon events obtained at the J/ψ resonance

a high effective mass as expected for the QED background.

Fig. 24

The three photon events measured at the ψ' resonance plotted as a function of the lowest and the highest effective mass found in each event
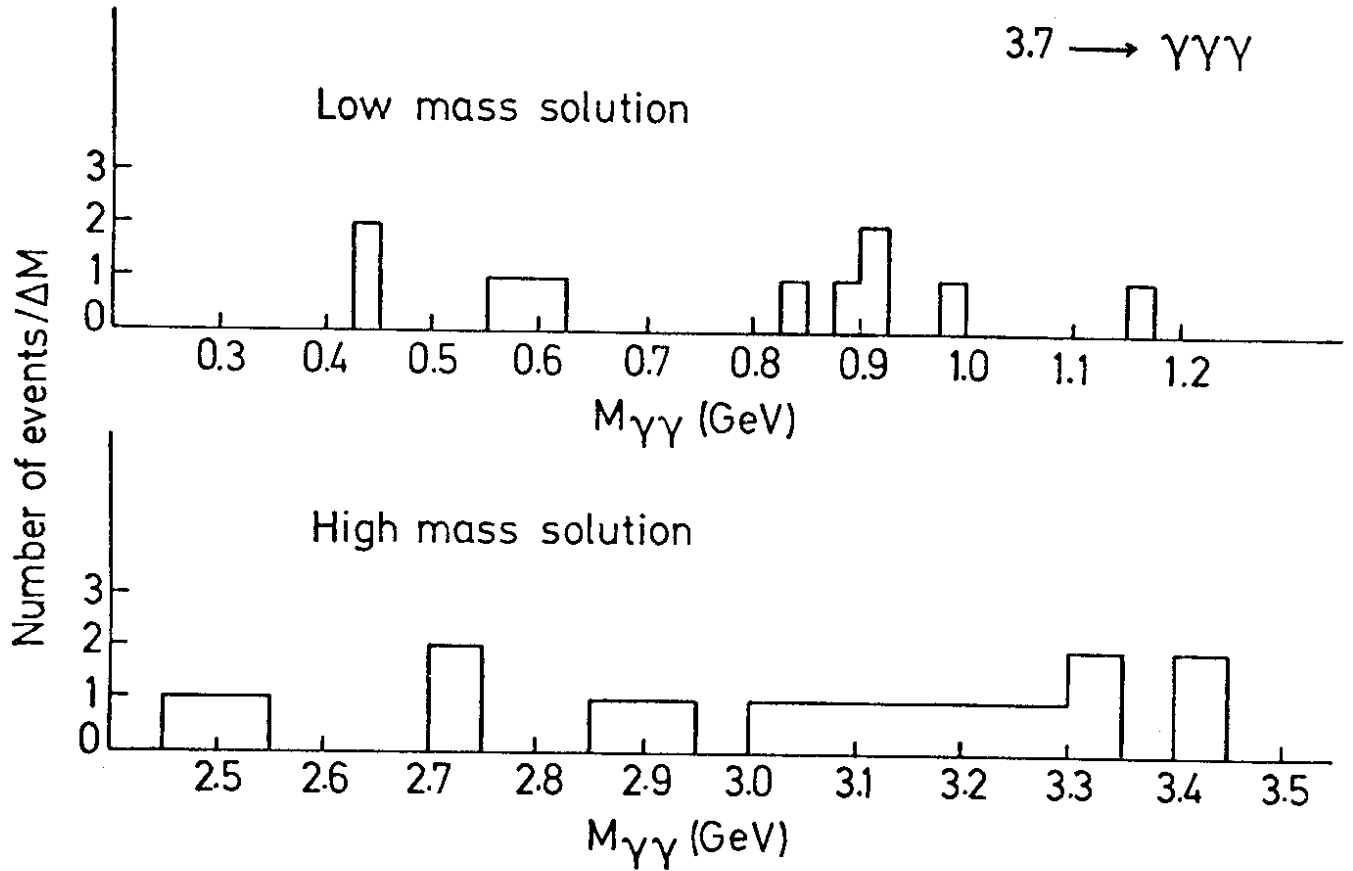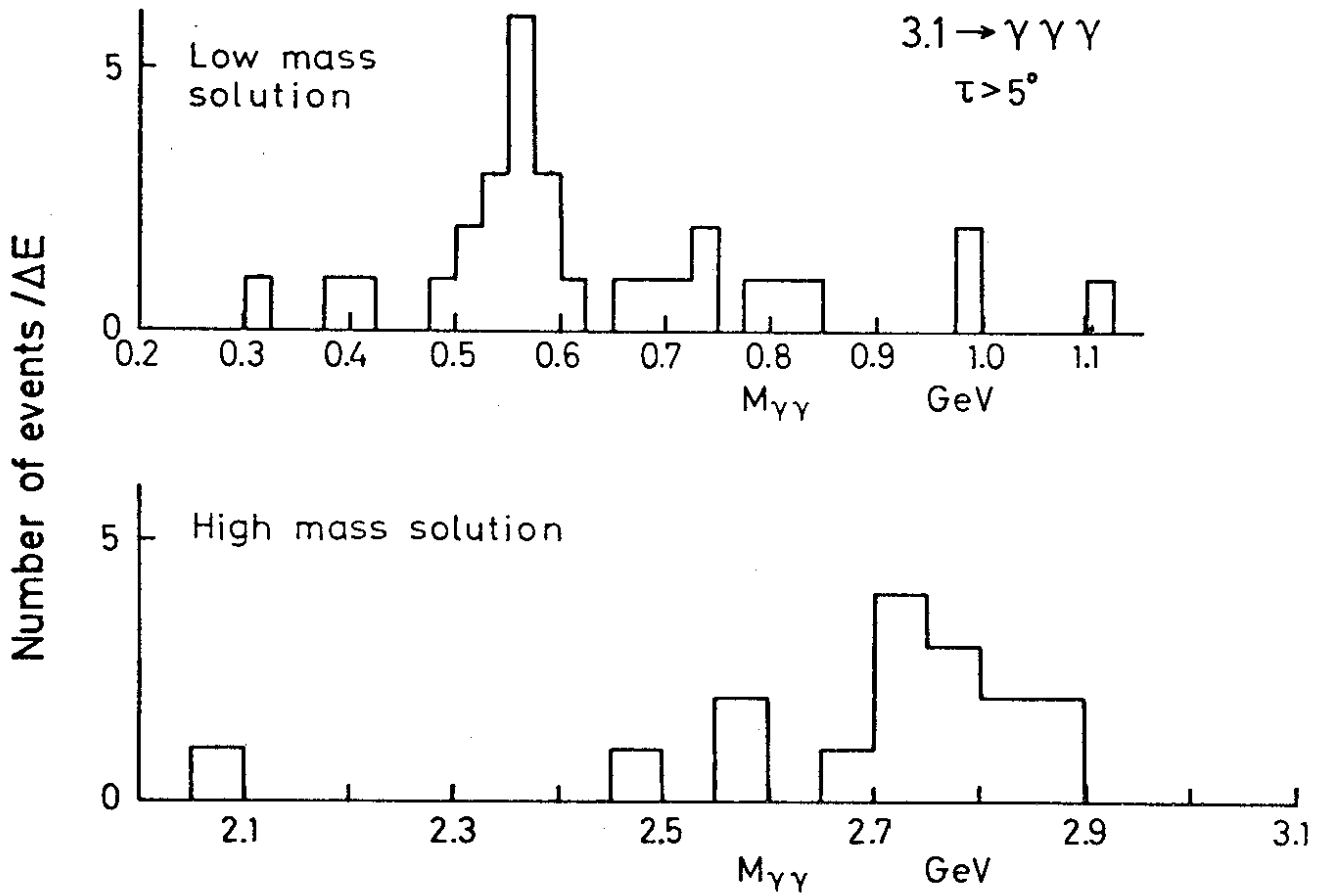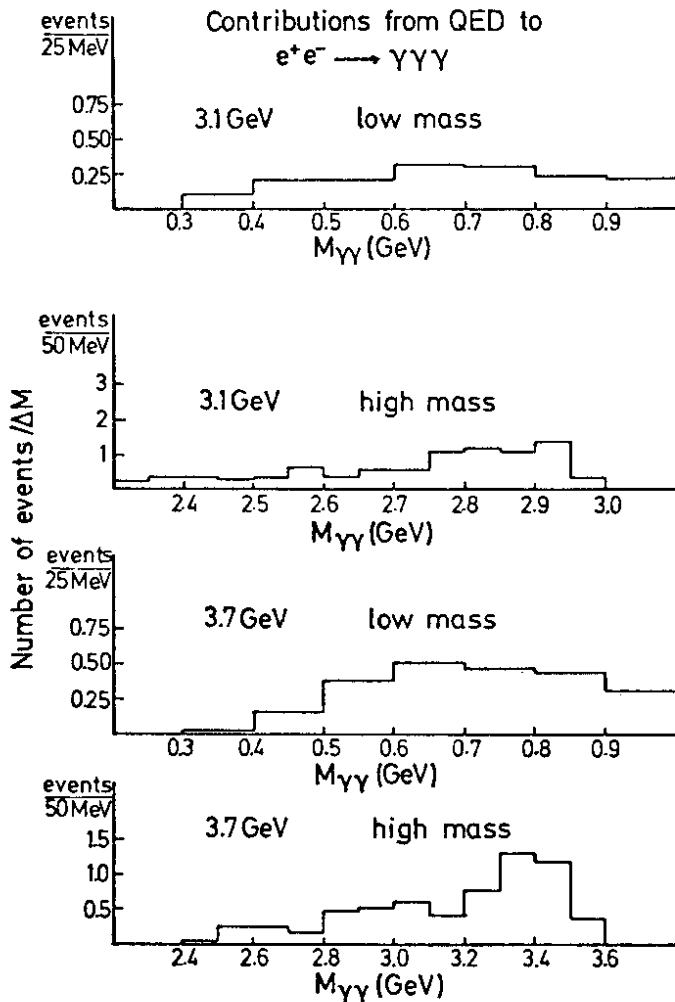
Fig. 25
The three photon events measured at the J/ψ resonance
plotted as a function of the lowest and the highest
effective mass found in each event. Events with the
low (or intermediate) effective mass within ± σ of
the mass of an η or η' are removed from the plot.

At the J/ψ mass a clear η signal is seen whose width is consistent with
the width expected from the experimental resolution alone. There are
two events at the mass of the η'. In the high mass solution there is a
clustering of events around a mass of 2.8 GeV. These events might result
from the decay of a new resonance X into a pair of photons. Note that a
width of ± 50 MeV is expected from the experimental resolution alone for
such a resonance. There is a cutoff in effective mass due to the loss
of photon detection efficiency at low photon energies. The mass accep-
tance, however, is uniform up to a mass of 3 GeV, so the observed peak
is therefore not caused by the folding of a decreasing mass acceptance
with a rapidly increasing QED cross section.

The three photon channel has a large background resulting from $e^+e^- \to \gamma\gamma\gamma$ via the QED diagrams. This background must be estimated and subtracted in order to assess the significance of the peak and to extract branching ratios. This was done as follows:

The energies (and therefore the angles) of the photons in a QED event were computed using the matrix elements for this reaction given by Berend and Gastman[18] as an input to the Monte Carlo computation. The probability for detecting the event was then evaluated with shower program and the known photon acceptance of the detector. The events so produced and detected were evaluated using the normal three photon analysis program with cuts identical to those applied to the real events.

The low and high mass distributions predicted as outlined above for the QED events are plotted in Fig. 26 for both CMS energies. Note the different binning used to plot the low and the high mass solution. The cross section for QED production increases with decreasing energy of one of the photons. This is reflected in the peaking of the cross section observed at high effective masses and the low background around the

Fig. 26
The rate for $e^+e^- \to \gamma\gamma\gamma$ predicted from QED alone. Plotted is the low mass and the high mass distribution of the events at the ψ' and the J/ψ resonance properly normalized.

mass of the η or the η'.

At CMS energies away from the resonances the QED process is expected to make the largest contribution to the observed three photon yield. In this experiment 4 events were found at energies outside the resonances, as compared to 4.8 events predicted by the Monto Carlo calculation.

At the ψ' resonance 15 events were observed as compared to 12.9 events expected from the QED process alone. The number of observed events is therefore consistent with the number predicted from QED production alone and only upper limits to the various decay modes can be given.
These limits were derived as follows: The background from QED was neglected and all events within ± σ of the appropriate mass value were assumed to result from the decay considered. The limits so derived multiplied by a factor of two are listed in Table VI below.

<div align="center">TABLE VI:</div>

Decay	Limit
$\psi' \to \eta\gamma$	$\int \sigma\, dE < 4.9$ nb MeV
	$\dfrac{\Gamma_{\eta\gamma}}{\Gamma} < 1.3 \times 10^{-3}$
$\psi' \to \eta'\gamma$	$\int \sigma\, dE < 51$ nb MeV
	$\dfrac{\Gamma_{\eta'\gamma}}{\Gamma} < 1.4 \times 10^{-2}$
$\psi' \to X(2.8)\gamma$	$\int \sigma\, dE < 1.3$ nb MeV
	$\dfrac{\Gamma_{X\gamma}}{\Gamma} \cdot \dfrac{\Gamma_{X\to\gamma\gamma}}{\Gamma_X} < 3.7 \times 10^{-4}$
$\psi' \to P_c(3.5)\gamma$	$\int \sigma\, dE < 0.48$ nb MeV
	$\dfrac{\Gamma_{P_c\gamma}}{\Gamma}\, \dfrac{\Gamma_{P_c\gamma}}{\Gamma_{P_c\to all}} < 1.3 \times 10^{-5}$

From the measured branching ratio of the decay $\psi' \to P_c + \gamma \to J/\psi + \gamma\gamma$ a lower limit $\Gamma_{P_c\gamma}/\Gamma > 4 \times 10^{-2}$ can be derived. This leads to an upper limit on the branching ratio of $P_c \to \gamma\gamma$: $\Gamma_{P_c\to\gamma\gamma}/\Gamma_{P_c} < 3.2 \times 10^{-3}$.

Of the 30 events observed at the J/ψ resonance 8.9 events were predicted to be QED events. The following results were obtained:

$J/\psi \to \eta \gamma$. 14 candidates for this decay were found as compared to 0.9 event predicted from QED. This corresponds to an integrated cross section of (16.6 ± 5.0) nb MeV and a partial width $\Gamma_{\eta\gamma} = (95 \pm 29)$ eV.

For the decay $J/\psi \to \eta'\gamma$ an upper limit on $\Gamma_{\eta'\gamma}$ is derived. We find $\Gamma_{\eta'\gamma} < 450$ eV. From these values

$$\frac{J/\psi \to \eta'\gamma}{J/\psi \to \eta\gamma} < 5 .$$

At a mass between 2.65 GeV and 2.85 GeV 10 events, compared to a predicted QED background of 3.4 events were found. An independent upper limit to background can also be evaluated from the measurements at the ψ' resonance assuming that all these events are from QED. This leads to an expected background of about 3 events in the mass range between 2.65 GeV and 2.85 GeV. Thus both methods of evaluating the QED background indicate an excess of events in this mass region. These events might result from the two photon decay of a new resonance with even charge conjugation and a mass around 2.75 GeV - 2.8 GeV.

The decay $J/\psi \to \gamma \gamma \gamma$ has also been investigated by the DESY-Heidelberg collaboration[19] using a large non-magnetic detector. Their findings are in good agreement with the results of the DASP group; in particular they also find a clustering of events at masses between 2.65 GeV and 2.85 GeV. The combined data and their statistical significance will be discussed by Prof. Heintze.

We have also searched for the decay $J/\psi \to X + \gamma \to p\bar{p} + \gamma$ by observing $p\bar{p}$ pairs with the magnets in coincidence with a photon in the inner detector. Two candidates for this decay were found with the photon in the plane defined by the $p\bar{p}$ pair. The invariant masses of the $p\bar{p}$ pairs were 2.784 GeV and 2.815 GeV.

We therefore tentatively conclude that we have observed a new resonance which we name X. This resonance decays with a branching ratio

$$\frac{J/\psi \to \gamma}{J/\psi \to \text{all}} \cdot \frac{X \to \gamma\gamma}{X \to \text{all}} \sim 1.5 \cdot 10^{-4}$$

into two photons. The decay $X \to p\bar{p}$ might also have been observed with a similar branching ratio.

I thank all the members of the DASP collaboration for a most enjoyable year.

REFERENCES

1) J.J.Aubert et al., Phys.Rev.Lett. 33, 1404 (1974)

   J.E.Augustin et al., Phys.Rev.Lett. 33, 1406 (1974)

   G.S.Abrams et al., Phys.Rev.Lett. 33, 1453 (1974)

2) DASP Collaboration, Phys.Lett. 53B, 393 (1974)

   DASP Collaboration, Phys.Lett. 56B, 491 (1974)

   G.Wolf, Rapporteur talk at the EPS Int. Conference on High
   Energy Physics, Palermo, Italy, June 1975

3) A.M.Boyarski et al., Phys.Rev.Lett. 34, 1357 (1975)

   V.Lüth et al., SLAC-PUB 1617, LBL-4211 - August 1975

4) The following Institutions and physicists are involved in the DASP-
   collaboration:
   W.Braunschweig, U.Martyn, H.G.Sander, D.Schmitz, W.Sturm, and W.Wallraff,
   I.Physikalisches Institut der RWTH Aachen,
   K.Berkelman, D.Cords, R.Felst, E.Gaderman, G.Grindhammer, H.Hultschig,
   P.Joos, W.Koch, U.Kötz, H.Krehbiel, D.Kreinick, J.Ludwig, K.-H.Mess,
   K.C.Moffeit, A.Petersen, G.Poelz, J.Ringel, K.Sauerberg, P.Schmüser,
   G.Vogel, B.H.Wiik, and G.Wolf - Deutsches Elektronen-Synchrotron DESY
   and II. Institut fpr Experimentalphysik der Universität Hamburg,Hamburg,
   G.Buschhorn, R.Kotthaus, U.E.Kruse, H.Lierl, H.Oberlack, K.Pretzl,
   and M.Schliwa - Max-Planck-Institut für Physik und Astrophysik,München,
   S.Orito, T.Suda, Y.Totsuka and S.Yamada, University of Tokyo, Tokyo.

5) L.Criegee, H.C.Dehne, J.Fox, G.Franke, G.Horlitz, G.Knies, E.Lohrmann,
   R.Schmitz, T.N.Ranga Swamy, U.Timm, P.Waloschek, G.G.Winter, S.Wolff,
   W.Zimmermann
   Contribution to the 1975 International Conference on Lepton and Photon
   Interactions at High Energies, Stanford, Calif. - USA

6) G.S.Abrams et al., Phys.Rev.Lett 34, 1181 (1975)

7) C.C.Morehouse - Talk at the April 1975 Washington APS Meeting
   Bull.Am.Phys.Soc. 20, 649 (1975) and
   The SLAC Summer Institute on Particle Physics, August 1975

8) M.K.Gaillard, B.W.Lee and J.L.Rosner, Rev.Mod.Phys. 47, 277 (1975)

9) For a recent review see:
   O.W.Greenberg,University of Maryland - Technical Report No. 75-064
   (1975) and references given in this report

10) The results on the decays $J/\psi \to \pi^+\pi^-$, K^+K^-, $p\bar{p}$ have been published
    DASP Collaboration, Phys. Lett. 57B, 297 (1975)

11) M.Bernardini et al., Phys.Lett. 46B, 261 (1973)

REFERENCES CONTINUED:

12) The existence of this state was first announced at the International
School of Subnuclear Physics, Erice, July 1975

DASP Collaboration Phys.Lett. 57B, 407 (1975)

13) G.J.Feldman et al., SLAC PUB-1621, LBL-4220

14) C.G.Callan et al., Phys.Rev.Letters 34, 52 (1975)

T.Appelquist et al., Phys.Rev.Letters 34, 365, (1975)

E.Eichten et al., Phys.Rev.Letters 34, 369 (1975)

15) J.W.Simpson, Phys.Rev.Lett. 35, 699 (1975)

16) Results obtained with a fraction of the present data have been
published
DASP Collaboration 53B, 491 (1975)

17) E.Pelaquier and F.M.Renard
Preprint Départment de Physique Mathématique
U.S.T.L., 34060 Montpellier, Cedex, France

18) F.A.Berend and R.Gastman - Nuclear Physics B61, 414 (1973)

19) J.Heintze - Paper presented at the 1975 Lepton Photon Symposium,
Stanford.